Circuitry and Function of the Dorsal Cochlear Nucleus

Eric D. Young and Kevin A. Davis
Department of Biomedical Engineering and Center for Hearing Sciences
Johns Hopkins University, Baltimore, MD 21205

Running title: Circuitry and Function of the DCN

To be published in Oertel, D., Popper, A.N., and Fay, R.R. (eds) *Integrative Functions in The Mammalian Auditory Pathway* New York: Springer-Verlag, 2001.

Send Correspondence to: Eric D. Young, Ph.D.
Department of Biomedical Engineering
Johns Hopkins University
720 Rutland Avenue/505 Traylor Research Building
Baltimore, MD 21205
(410) 955-3162 (work)
(410) 955-1299 (FAX)
eyoung@bme.jhu.edu

1. Introduction

In Chapter 2 of this volume, Smith and Spirou describe the wonderful complexity of the brainstem auditory system. This system forms a collection of parallel pathways which diverge at the first auditory synapse in the brainstem, in the cochlear nucleus (CN), and then converge again, at least in a gross anatomical sense, in the inferior colliculus. The CN is a well-studied collection of neural circuits that are diverse both in anatomical and physiological terms (reviewed by Cant 1992; Rhode and Greenberg 1992; Young 1998). These vary from the simplest system, the bushy cells of the ventral cochlear nucleus (VCN; see Yin, Chapter 4), to the most complex, in the dorsal cochlear nucleus (DCN). The DCN differs from other parts of the CN by having an extensive internal neuropil formed by groups of interneurons (Lorente de Nó 1981; Osen et al. 1990). As a result, the DCN makes significant changes in the auditory representation from its inputs to its outputs. In this chapter, the neural organization of the DCN is reviewed, paying most attention to data from the cat. The response properties of DCN neurons are discussed in the context of its neural organization and related to data on the functional role of the DCN in hearing.

2. Role of the dorsal cochlear nucleus in hearing

Understanding auditory processing in terms of the neural circuits in the brain depends on working out the roles of the multiple parallel pathways of the brainstem auditory system. An excellent example is provided by Chapter 4 of this book (see Yin, Chapter 4), in which the role of the system consisting of the bushy cells in the CN and the principal cells of the superior olivary complex is described. This circuit makes the precise comparisons of time of arrival and sound level in the two ears that are needed for binaural sound localization. In this chapter, the role of a second CN pathway, that formed by the principal cells of the DCN, is discussed.

By the “role” of the DCN, we mean the computations done by the DCN for the other parts of the auditory system. This is an ill-defined concept in that there is no accepted method for defining the role of an arbitrary group of neurons in the brain. Several kinds of evidence can be offered. First, there is behavioral evidence, i.e. the appearance of deficits in certain kinds of auditory performance when the neurons are lesioned. Using an example from the previous chapter (see Yin, Chapter 4), deficits in sound localization performance are seen when lesions are made in the principal nuclei of the superior olivary complex (Kavanagh and Kelly 1992; van Adel and Kelly 1998). Second, there is evidence from the projection sites of the principal cells of the nucleus. Again, using the example of the previous chapter, the bushy cells of the CN project essentially only to the superior olivary complex and are the primary source of inputs to the superior olive’s principal nuclei. This fact means that CN bushy cells are the pathway through the CN for information about binaural cues for sound localization. Third, there is evidence from the response properties of the neurons. The responses may convey information about a particular aspect of the stimulus (e.g. Blackburn and Sachs 1990; Dabak and Johnson 1992) or respond to the stimulus in a way that corresponds well to some aspect of perception (e.g. Cariani and Delgutte 1996a,b; May et al. 1996). In either case, the responses are prima facie evidence that the neurons are participating in the corresponding aspect of auditory processing. Again a clear

example is provided by the bushy cell/superior olivary circuit (see Yin, Chapter 4). The superior olive is the first place in the auditory system where neurons respond sensitively to differences between the stimuli at the two ears, which argues that performing the basic calculations for binaural sound localization is the principal role of this structure.

Each of the three kinds of evidence has its own problems of interpretation. Strong conclusions can be drawn only when multiple lines of evidence converge to support the same set of hypotheses. In this chapter, we will focus mainly on the third kind of evidence for the case of the DCN, but the existing evidence of the first two kinds will be reviewed first.

The principal cells of the DCN project directly to the central nucleus of the inferior colliculus (CNIC; Osen 1972; Oliver 1984; Ryugo and Willard 1985). They are unique in the CN in that their activity reflects substantial interneuronal processing in the complex neuropil of the DCN (Lorente de Nó 1981; Berrebi and Mugnaini 1991; Weedman et al. 1996). They are also unique in that they serve as the convergence point for auditory and somatosensory information (Young et al. 1995). The main features of the interneuronal circuitry of the DCN have been worked out, so that the generation of DCN principal cell responses to sound and somatosensory stimuli is well understood. These results suggest that one role of the DCN is to process the complex spectral patterns produced by directionally dependent filtering in the external ear (Young et al. 1992; Imig et al. 2000). These so-called head-related transfer functions (HRTFs) convey information about sound localization (e.g. in the cat, Musicant et al. 1990; Rice et al. 1992). Thus one hypothesis for the role of the DCN in the auditory system is to process aspects of spectral sound localization cues. This chapter will review what is known about neural signal processing in the DCN, as it relates to this hypothesis.

2.1 Evidence from behavioral studies of sound localization

Because the output axons of the DCN leave the nucleus through the dorsal acoustic stria (DAS; Fernandez and Karapas 1967; Adams and Warr 1976), which is separate from the other outputs of the CN, it is possible to interrupt the DCN's output with minimal effects on the projections from the rest of the CN. The intermediate acoustic stria, containing axons of multipolar cells in VCN (Adams and Warr 1976), is near the DAS and is probably damaged when the DAS is cut, but the largest output of the VCN, which passes through the trapezoid body, is unaffected. A surprising result from experiments in animals with DAS lesions is that the deficits produced are subtle. Masterton and colleagues showed that DAS lesions did not affect cats' absolute thresholds, masked thresholds, or ability to discriminate the location of a sound source (Masterton and Granger 1988; Masterton et al. 1994; Sutherland et al. 1998a).

The only reported positive finding from such experiments is that lesioned cats show a deficit in sound localization when tested in situations that require pointing to the actual location of the sound source. This is to be distinguished from situations in which the cat is asked to discriminate the location of two speakers, a task that can be done without necessarily knowing where either speaker is located. The deficit in sound localization has been shown in two ways: First, Sutherland and colleagues used untrained cats performing a reflex head orientation to a sound source (Sutherland et al. 1998b). The accuracy of the orientation was decreased after a

DAS lesion. Second, May trained cats to point to the source of a sound by turning their heads (May 2000). Although the results are complex, DAS lesions produced a clear deficit in performance, especially for the vertical component of localization. When the same cats were tested in speaker discrimination, however, they showed little or no deficit, consistent with results from Sutherland and colleagues mentioned above.

2.2 Sound localization cues in the cat

Interpretation of the DCN's role in sound localization depends on understanding the nature of sound localization cues in the cat. Figure 1 shows a summary of the relevant aspects of these cues. Figures 1A and 1B show examples of HRTFs from a cat. These functions show the magnitude of the frequency-dependent gain from a speaker in free field to a microphone near the eardrum (Musicant et al. 1990; Rice et al. 1992). That is, they show the changes in a sound's spectrum that are produced by the acoustical effects of the head and external ear. If a speaker were to produce a broadband noise with a flat spectrum, i.e. equal energy at all frequencies, the signal at the cat's eardrum would have a spectral shape equal to the appropriate HRTF. The important point for the present discussion is that HRTFs are direction-dependent. Figure 1A shows HRTFs with the sound source at three different azimuthal positions; that is, the source was moved in 30˚ steps along the horizon. The

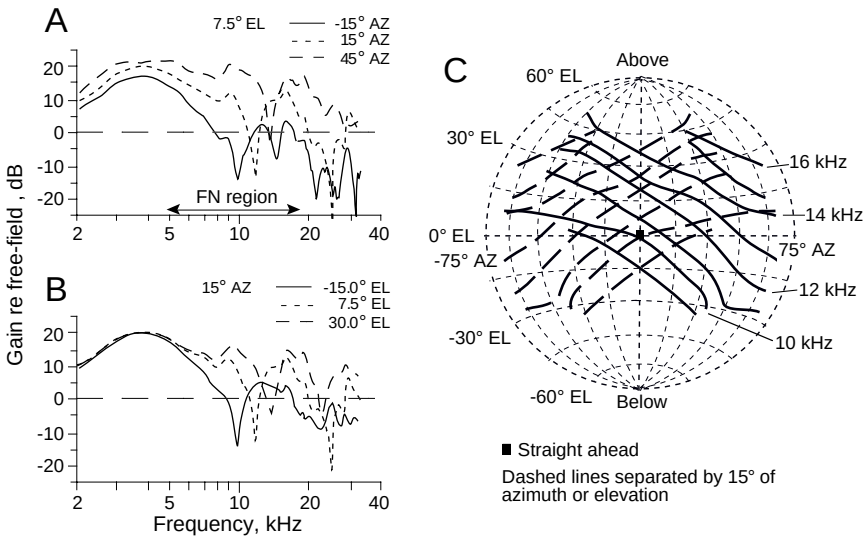

Figure 1. Characteristics of head related transfer functions (HRTFs) in the cat. These functions show the ratio between the amplitude of a sound at a microphone near the cat's eardrum and the amplitude of the sound at the same point in space in the absence of the cat. They thus measure the effect of the cat's head and external ear in perturbing the sound field. A. HRTFs for three different azimuths at fixed elevation, i.e. moving parallel to the horizon in a left-right direction. Azimuth and elevation are defined below. B. HRTFs for three elevations at fixed azimuth, i.e. moving in a down to up direction. In both A and B, notice the prominent notches in the transfer functions at frequencies between 8 and 17 kHz (first notch or FN). C. Contours of constant first-notch frequency for locations in space in front of a cat. Light dashed lines show contours of constant azimuth and elevation. Each heavy line shows all the speaker locations for which there would be a first notch of a certain frequency in one ear. Solid lines are for the right ear and dashed lines are for the left ear; left ear contours are actually just mirror images of the right ear contours, assuming symmetric ears. *Azimuth* refers to positions along the horizon: 0˚ is straight ahead and positive azimuths are for positions on the right, where the measuring microphone was located. For example, a speaker at 20˚ azimuth is centered on a line which makes a 20˚ angle with respect to straight ahead. *Elevation* refers to vertical positions and is measured with respect to the horizon; 0˚ elevation is on the horizon, positive elevations are above the horizon. (Redrawn from Rice et al. 1992 with permission.)

HRTFs at these locations differ in two important ways. First, the overall gain of the HRTF is higher at the larger azimuths. This is most clearly seen at frequencies below 8 kHz, where the HRTFs are smooth in shape. The change in gain means that the sound is louder as the source moves toward the ear; this effect produces a difference in interaural sound level, called an interaural level difference (ILD), as the sound source moves away from the midline. For example, if the speaker were located at 15˚ azimuth, the HRTF for 15˚ would apply to the right ear and the HRTF for –15˚ would apply to the left ear. The ILD would be the (frequency dependent) difference between these two HRTFs.

The second difference in HRTFs with azimuth is a difference in their detailed spectral shapes. The most obvious shape change is the movement in the center frequency of the prominent spectral notch located in the frequency region between 5 and 18 kHz (marked “FN region” in Fig. 1A). The center frequency of the notch increases as the azimuth increases. This notch, called the first notch, is a potent spectral cue to sound source location (Rice et al. 1992). At higher frequencies, there are more complex and variable changes in the spectral cues.

Figure 1B shows HRTFs from three different elevations at the same azimuth. Similar changes in spectral shape are seen, with the first notch frequency increasing with elevation, Note, however, that the overall gain does not change at low frequencies. Apparently the principal cue to elevation is spectral shape.

Accompanying the differences in interaural level and spectral shape is a difference in the time of arrival of the stimuli at the two ears, an interaural time difference (ITD), which is not shown in Fig. 1 (Roth et al. 1980; Kuhn 1987). Psychophysical analysis of humans and cats have shown that all three cues to sound localization are used (reviewed by Middlebrooks and Green 1991 and Populin and Yin 1998). Spectral cues are most important, in human observers, for elevation and for discriminating front from back.

In cat, the first-notch frequency is a potential spectral cue for both azimuth and elevation. Figure 1C shows a plot of the distribution of first-notch frequencies for locations in front of a cat. The lines show contours of constant first-notch frequency, i.e. locations in space having the same first-notch frequencies. The solid lines show contours for the right ear and the dashed lines show contours for the left ear (assumed to mirror the right ear data). This plot shows that a cat can localize a sound over a significant region of space based on a knowledge only of the first-notch frequencies in the two ears.

If cats do use the first-notch cue to localize sound, then their sound localization performance should be sensitive to manipulations that interfere with the first-notch information. Huang and May (1996a) trained cats to localize sounds from speakers in the frontal field, i.e. roughly over the range of locations shown in Fig. 1C. The cats were trained with broadband noise, so that all the spectral cues were present, along with the interaural cues (ILD and ITD). The cats were required to respond by making a head orientation to the sound source, to guarantee that the task involved actually localizing the sound. Cats were tested with tones and with filtered bands of noise. Their performance was best when the stimulus contained noise in the frequency band between 5 and 18 kHz. Because this is the frequency region where the first notch cue is located, this result suggests that cats depend on the first notch cue for sound localization.

In an additional experiment, cats were trained to discriminate the sounds coming from two different speakers (Huang and May 1996b). Again the cats were trained with broadband noise and tested with noise filtered to remove certain frequency bands. In this case, removing the signal energy above 18 kHz had the largest effect on performance, suggesting that the cats depended on changes in the stimulus spectrum at high frequencies to discriminate speakers. Apparently, cats can hear the spectral cues at higher frequencies and discriminate changes in the spectrum, but the variation of spectral shape with sound source direction is so complex at high frequencies that it cannot easily be used as a cue for sound location.

The apparent difference between the cues that cats use for sound localization versus direction discrimination is consistent with the behavioral results, discussed above, suggesting that the DCN is involved in sound localization, but not in direction discrimination. The shape of the signal spectrum at the eardrum is represented multiple times in the output pathways of the CN; for example, the chopper neurons of the VCN provide a robust representation of spectral shape for vowel-like stimuli (Blackburn and Sachs 1990), and so probably also provide a good representation of the spectral shapes created by HRTFs. Evidence will be summarized below to show that DCN principal cells give a strong inhibitory response to spectral notches; this response is a specialized mechanism in the DCN that is not present in VCN. Thus, it is possible that the outputs of the VCN are sufficient to support discrimination behavior, so that this behavior is not affected by DAS lesions, whereas the outputs of the DCN are necessary for reflex orientation and sound localization. The existence of the notch response in DCN principal cells provides evidence that the DCN is involved in processing spectral sound localization cues and ties the behavioral and lesion data together.

2.3 Evidence from the targets of efferent projections from the DCN

The axons of DCN principal cells project mainly to auditory targets in the CNIC, bypassing the superior olive and the nuclei of the lateral lemniscus (Fernandez and Karapas 1967; Osen 1972; Ryugo and Willard 1985). The effects of DCN activity on cells in CNIC is beginning to be understood and this topic will be discussed in the last section of this chapter. However, knowledge about the targets within CNIC of DCN axons is in a preliminary state, and it is not possible to draw strong conclusions about the DCN's role from its projection to CNIC.

One intriguing hypothesis is that there are DCN-like or DCN-related subsystems of the auditory system which exist in the inferior colliculus, medial geniculate, and auditory cortex. Imig and colleagues have argued for the existence of such subsystems based on cells in thalamus and cortex that are sensitive to monaural (and therefore spectral) sound localization cues, as opposed to binaural cues (Samson et al. 1993; Imig et al. 1997). Further evidence for a segregation of DCN outputs is provided by the finding that evoked potentials produced by electrical stimulation of the DAS are larger and shorter in latency in the anterior auditory field than in the primary auditory cortex of the cat (Imig and Samson 2000). The existence of a separate DCN-related module of cells in CNIC is suggested by the response characteristics of CNIC neurons (Ramachandran et al. 1999) and by the effects on CNIC neurons of blocking the DAS with lidocaine (K.A. Davis, unpublished); this evidence will be reviewed in the last section of this chapter.

The DCN projects to non-auditory structures, among them the caudal pontine reticular nucleus (Lingenhöhl and Friauf 1994); this nucleus is important for acoustic startle reflexes, and the DCN has been shown to contribute a component of startle (Meloni and Davis 1998). These data do not provide much insight into the auditory role of the DCN, however, because the nature of auditory processing in the startle reflex has not been analyzed. For example, it would be useful to know if there are late components of startle that require auditory processing, such as a knowledge of the location of the sound source that induced the startle.

3. Structural organization of neural circuits in the DCN

Figure 2A is a sketch of a frontal section of the cat DCN, showing the main principal cell types and some of the interneurons of the nucleus. The DCN consists of three layers which are cut in cross section in this figure. The layers are organized around the pyramidal cells, principal cells whose cell bodies form the second layer (Blackstad et al. 1984), along with the cell bodies of granule cells (Mugnaini et al. 1980b). The principal cells' somata are shown as black shapes in Fig. 2A; the prominent layer of pyramidal cell bodies running parallel to the surface of the nucleus is evident. A full drawing of one pyramidal cell is shown (*P*). These cells are bipolar, with an apical dendritic tree extending into the molecular layer, i.e. toward the free surface of the nucleus, and a basal dendrite ex-

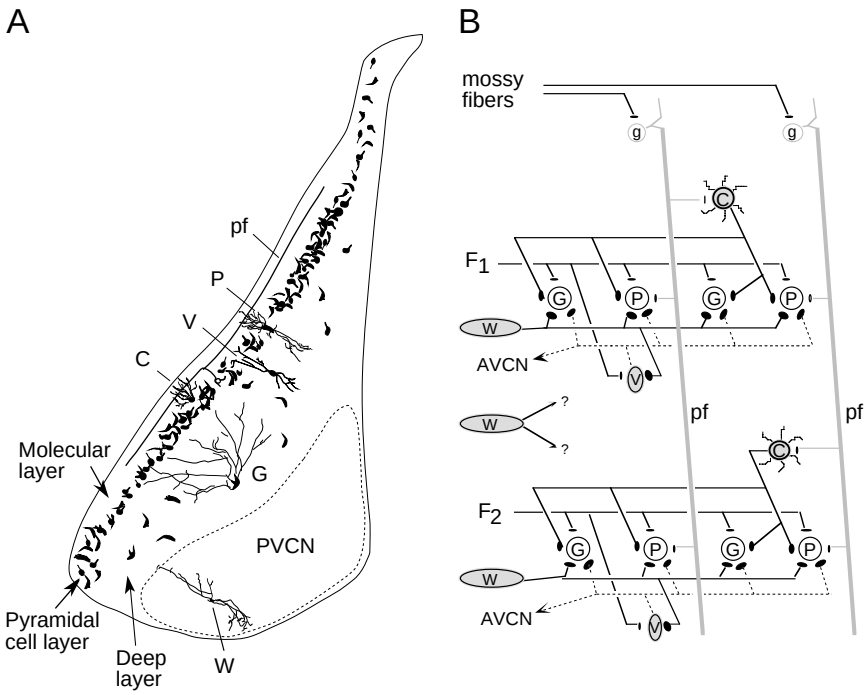

Figure 2. A. Sketch of a frontal section of the DCN showing the positions of the cell types that will be discussed in this chapter. The section has roughly the shape and layout of the cat DCN, although the drawing is a combination of descriptions from both cat and rodent. The dark shapes are somata of DCN principal cells (pyramidal and giant cells) antidromically filled from an injection of HRP in the CNIC (based on drawings in Ryugo and Willard 1985). Drawings of individual examples of six cell types are shown to illustrate the typical positions of their cell bodies and dendritic trees in the DCN and VCN. The layers are identified at bottom left. The axon of one granule cell is shown forming a parallel fiber (*pf*) in the molecular layer; the axon originates in a granule cell in the pyramidal cell layer. B. Schematic circuit diagram of the DCN, drawn in a plane parallel to the layers of the nucleus. F_1 and F_2 represent excitatory inputs from auditory nerve fibers and perhaps VCN T-multipolar neurons with best frequencies F_1 and F_2, forming two isofrequency sheets. Excitatory connections are unfilled, inhibitory neurons are shaded and have filled terminals. Abbreviations for cell types: *g* – granule; *C* – cartwheel; *G*- giant; *P* – pyramidal; *pf* – parallel fiber; *V* – vertical; *W* – wideband inhibitor (VCN D-multipolar or radiate neuron). (A is drawn from figures in Osen 1969; Osen 1983; Rhode et al. 1983; Ryugo and Willard 1985; Smith and Rhode 1989; Osen et al. 1990; and Berrebi and Mugnaini 1991.)

tending into the deep layer.

The superficial, or molecular, layer lies above the pyramidal cell somata. It contains the apical dendritic trees of pyramidal cells as well as several kinds of interneurons, including the inhibitory cartwheel (*C*), Golgi, and stellate cells, and their associated neuropil. The cartwheel cell somata are scattered in a thick layer extending from the pyramidal cell layer into the molecular layer (Berrebi and Mugnaini 1991). Stellate cells are not shown in Fig. 2A, but are located in the superficial layer (Wouterlood et al. 1984) and Golgi cells, also not shown, are located in the granule cell regions (Mugnaini et al. 1980a). The inputs to the molecular layer are parallel fibers (*pf*), which are the axons of granule cells. Parallel fibers run roughly parallel to the plane of the frontal section shown in Fig. 2A, and make synapses on the interneurons and principal cell dendrites located in the molecular layer. Granule cell somata are concentrated in the pyramidal cell layer of the DCN and in six other areas mostly around the surface of the DCN and VCN (Mugnaini et al. 1980b). Inputs to the granule cells are made by mossy fiber terminals of axons originating from a variety of auditory and non-auditory sources (reviewed in Weedman and Ryugo 1996 and Wright and Ryugo 1996). Among the best studied of these are inputs from the somatosensory dorsal column and spinal trigeminal nuclei (here called MSN for medullary somatosensory nuclei; Itoh et al. 1987; Weinberg and Rustioni 1987), but additional inputs come from the vestibular system (Burian and Gestoettner 1988; Kevetter and Perachio 1989), from pontine nuclei (Ohlrogge et al. 2000), and probably also from other sources not yet described.

The deep layer of the DCN is a heterogeneous region located deep to the pyramidal cell bodies. It contains the basal dendritic trees of pyramidal cells along with the somata and most of the dendritic trees of the second DCN principal cell type, the giant cell (*G*). Giant cell somata can be seen as scattered large profiles in the deep layer in Fig. 2A. The deep layer also contains the vertical cells (*V*), also called tuberculoventral cells, whose somata are located deep to the pyramidal cells (Lorente de Nó 1981; Saint Marie et al. 1991; Zhang and Oertel 1993b). The main inputs to the deep layer are auditory axons, from the auditory nerve (Osen 1970; Ryugo and May 1993) and from VCN multipolar cells (Adams 1983; Smith and Rhode 1989; Oertel et al. 1990). Auditory nerve fibers travel roughly perpendicular to the plane of section in Fig. 2A. They innervate neurons along their path, forming isofrequency sheets of cells. The directions of travel of the parallel fibers in the superficial layer and the auditory nerve axons in the deep layer are roughly orthogonal. The dendritic trees of pyramidal cells, cartwheel cells, and vertical cells are flattened in the direction parallel to the auditory nerve fibers, so that these cells tend to receive inputs within a narrow range of frequencies (Osen 1983; Blackstad et al. 1984; Berrebi and Mugnaini 1991).

The arrangement of synaptic connections among the main neuron types of DCN is shown schematically in Fig. 2B. This figure shows a view of the DCN looking down on the surface, in the plane of the paper in Fig. 2A; the isofrequency sheets run from left to right and the parallel fibers run from top to bottom. Two isofrequency sheets are shown, for frequencies F1 and F2. The sheets are bound together by the axons of auditory nerve fibers and possibly also VCN multipolar neurons. Each sheet contains a complement of pyramidal (*P*) and giant (*G*) cells along with a vertical cell (*V*) representing the vertical cells in the sheet. The vertical cell axons distribute in parallel to isofrequency sheets and terminate on both principal cell types.

There are two cell types in VCN which send axon collaterals to the DCN (Smith and Rhode 1989; Oertel et al. 1990; Doucet and Ryugo 1997). The planar or T-multipolars are VCN principal cells whose axons travel to the CNIC in the trapezoid body. These neurons have dendritic trees oriented in the direction of the auditory nerve fibers and make terminals with excitatory morphology (asymmetric with round vesicles) in DCN. The radiate or D-multipolars are VCN principal cells whose axons probably leave the CN in the intermediate acoustic stria. Their dendrites are oriented across the array of auditory nerve fibers, so that they receive inputs from a broad range of frequencies. Radiate neurons are glycinergic (Doucet et al. 1999) and make terminals with inhibitory morphology in DCN. They correspond to the element called the wideband inhibitor (*W*) in Fig. 2. Evidence to associate the wideband inhibitor and the radiate neuron is discussed in a later section. Whether these neurons make tonotopic connections within an isofrequency sheet, as shown in Fig. 2B, is not settled; this uncertainty is indicated by the *W* neuron with projections ending in question marks.

The circuitry of the molecular layer of the DCN is represented in Fig. 2B by the mossy fiber inputs, granule cells, and cartwheel cells. Like other DCN circuits, cartwheel cell axons distribute predominantly in parallel with the isofrequency sheets, as they are drawn (Berrebi and Mugnaini 1991). Although no source of auditory inputs to cartwheel cells is shown in Fig. 2B, these cells do respond to sound (Parham and Kim 1995; Davis and Young 1997), so either some mossy fibers are auditory or there are additional connections that are not shown. Auditory nerve fibers do not terminate in the molecular layer (Merchán et al. 1985; Ryugo and May 1993).

The circuitry of the molecular layer is substantially more complex than is shown in Fig. 2B. Four additional cell types (Golgi cells, stellate cells, unipolar brush cells, and chestnut cells; Mugnaini et al. 1980a; Wouterlood et al. 1984; Weedman et al. 1996) have been described in the molecular layer. However, the details of their participation in DCN circuits have not been worked out from either the anatomical or physiological perspective.

4. Response properties of DCN neurons

The circuit diagram of Fig. 2B shows that the DCN is well-endowed with inhibitory interneurons. In fact, the responses to sound of DCN neurons display substantial inhibitory influences and, in the work discussed in this chapter, it has proven most useful to characterize responses in the DCN on the basis of the nature and extent of inhibitory inputs. Figure 3 shows typical response maps of elements of the DCN circuit. These maps are based on responses to tones of various frequencies and sound levels; they show discharge rate versus frequency at a series of fixed sound levels (actually attenuations, as explained in the figure caption). The horizontal line in each plot is the spontaneous discharge rate. Increases in rate above spontaneous are colored black, to show excitatory response regions; decreases in rate, inhibitory regions, are shaded.

Figure 3A shows a type IV response map, which is characteristic of most principal cells in the unanesthetized cat DCN (Young and Brownell 1976; Young 1980; Rhode and Kettner 1987). Type IV response maps vary considerably from neuron to neuron, but the one shown in Fig. 3A displays the characteristics that are most typical of this response type in decerebrate cat

(Spirou and Young 1991). There is a small excitatory area near threshold centered on the neuron's best frequency (BF, 17.5 kHz). At higher sound levels, the response near BF is inhibitory over a V-shaped area called the central inhibitory area (CIA, centered on 16-17 kHz in this case). The upper frequency edge of the CIA is bounded by a small excitatory ridge (near 22 kHz here). Usually there is another inhibitory area at higher frequencies, above 22 kHz in this example, and a large excitatory area at high levels and low frequencies, below 10 kHz in this example. Several examples of type IV response maps are given in subsequent figures in this chapter; these illustrate the variability in type IV maps. The only required features of a type IV map are the low-level excitatory area at BF and the CIA. A model for the type IV response map is presented below; quantitative variations in this model have been shown to be capable of producing the range of type IV response maps observed in the DCN (Reed and Blum 1995).

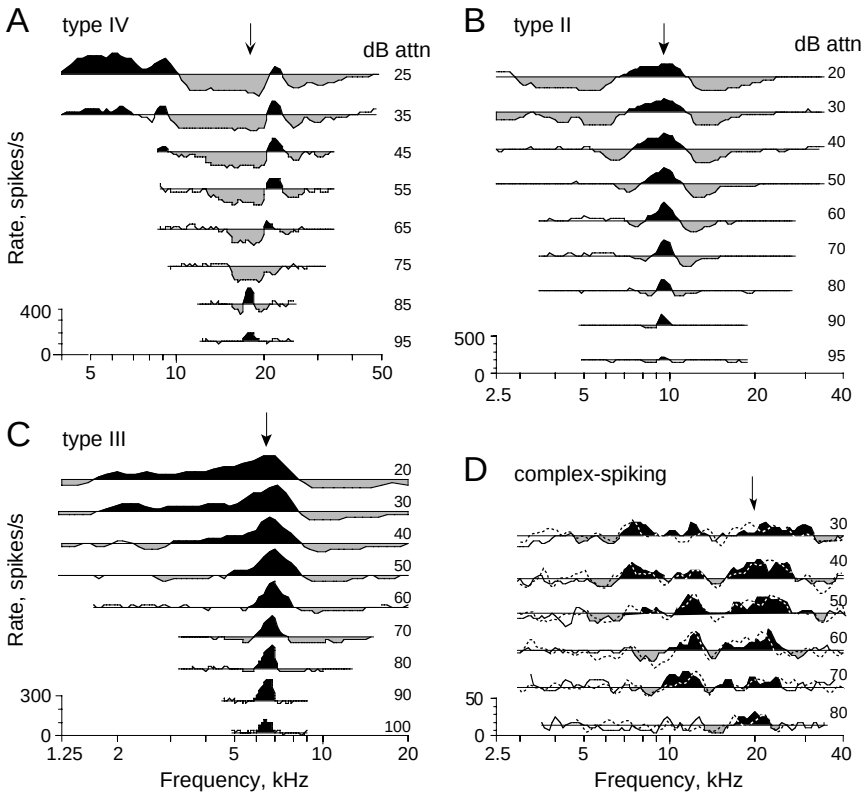

Figure 3. Response maps for DCN neurons. The maps are labeled at upper left with the corresponding response type. Each map is a collection of plots of discharge rate versus frequency obtained from the presentation of 100 tone bursts of duration 200 ms; the tone frequencies are interpolated logarithmically over a range varying from 1-4 octaves, as shown on the abscissa. For each plot, the attenuation was held constant at the value given by the number at the right of the curve. The actual sound level varies with the acoustic calibration, but 0 dB attenuation corresponds to roughly 100 dB SPL. The acoustic calibration is reasonably flat (e.g. Rice et al. 1995) and typically varies less than ±10 dB over the frequency range of a response map. The horizontal line in each plot is the spontaneous rate. The rate scale at lower left applies to the plot at the lowest sound level; other plots are shifted vertically to prevent overlap, but use the same rate scale. Arrows at the top point to the BFs. Type III and IV responses are recorded from principal cells (pyramidal and giant cells) and type II responses are recorded from vertical cells. The type II response map was constructed in the presence of a weak exciter tone of fixed level and frequency (9.35 kHz, 90 dB attn.) for the reasons described in the text. Complex-spiking units are recorded from cartwheel cells, which show widely varying response maps (Davis and Young 1997). For the example shown here, two repetitions of the map are superimposed (solid and dashed lines). (B redrawn from Spirou et al. 1999 and D redrawn from Davis and Young 1997 with permission.)

Type II responses (Fig. 3B) have a narrow V-shaped excitatory area centered on BF and a significant inhibitory surround. These units are characterized by two features in addition to their response maps: 1) type II units do not have spontaneous activity; and 2) type II units give weak or no response to

broadband noise (Spirou et al. 1999). Because of the lack of spontaneous activity, inhibitory responses are demonstrated in response maps like Fig. 3B by presenting a low-level BF tone of fixed attenuation and frequency; this tone produces a low rate of background activity against which both excitatory and inhibitory responses can be seen. Type II responses are recorded from vertical cells in DCN, based on the fact that they can be antidromically stimulated from the VCN where vertical cells project an axon collateral (Young 1980) and based on identification of type II neurons by dye filling (Rhode 1999).

Type III neurons (Fig. 3C) have response maps like those of type II units, with a central V-shaped excitatory area centered on BF and inhibitory sidebands. They are recorded from principal cells, and perhaps also other cell types (Young 1980). Type III responses differ from type II in that type III units have at least some spontaneous activity and respond to broadband noise about as strongly as they do to tones (Young and Voigt 1982). To discriminate type II and type III units, a spontaneous rate of 2.5 /s and a relative noise responsiveness (maximum driven rate to noise divided by maximum driven rate to BF tones) of 0.35 are typically used. Type III units are relatively rare in the decerebrate cat DCN (Shofner and Young 1985), but are much more common in anesthetized cats or in rodents like the gerbil, regardless of anesthetic state (Evans and Nelson 1973; Davis et al. 1996a; Joris 1998). Pentobarbital anesthesia converts type IV units to type III (Evans and Nelson 1973; Young and Brownell 1976), presumably by reducing the potency of the vertical cell inhibitory circuit. This issue is discussed in more detail below.

Two additional classes of DCN response maps are not shown in Fig. 3. Type IV-T units appear to be an intermediate between types III and IV. They are like type IV units, except with weaker inhibition in the CIA (Spirou and Young 1991). Type I/III units have no spontaneous activity and response maps like those of type II units. They differ from type II units in the quantitative details of their BF-tone responses and in that they respond strongly to broadband noise (Spirou et al. 1999). The criteria used to distinguish type II and type I/III units are somewhat arbitrary and it is clear that they show overlapping properties. However, there is an important functional difference between the two unit types, in that good evidence exists to associate type II responses with the vertical cell and with inhibitory inputs to principal cells (see below; Young 1980; Voigt and Young 1990; Rhode 1999), whereas there is no evidence that type I/III units serve an inhibitory function. There is also no evidence as to the identity of type I/III units.

The remaining response type in Fig. 3 is the complex-spiking neuron, whose response map is shown in Fig. 3D. Complex-spiking neurons are those whose action potentials, in extracellular recording, show short bursts of spikes. These bursts resemble the mixed calcium-sodium spike bursts recorded intracellularly in cartwheel cells (Zhang and Oertel 1993a; Manis et al. 1994; Golding and Oertel 1997). Such bursts are seen in extracellular recording only in the superficial DCN, at depths that correspond to the location of the cartwheel cell bodies (Parham and Kim 1995; Davis and Young 1997). Based on this evidence, we assume that complex-spiking responses are recorded from cartwheel cells. Complex-spiking neurons almost all respond to sound, but their responses are highly variable, as illustrated by the response map shown in Fig. 3D. Two repetitions of the map are shown (solid and dashed lines); the variability between these two is typical of complex-spiking neurons. These neurons also typically show

fluctuations in their spontaneous rates and it is often hard to assign them a BF. Their response maps show a mixture of excitatory and inhibitory areas, but these are not organized in any typical patterns.

The characterization of type IV units provided by tone response maps suggests that these units respond to stimulus energy in a mainly inhibitory fashion. However, when broadband noise is used as the stimulus, the conclusion is different. Figure 4 shows responses to broadband noise and to noise notches for two type IV units. The response maps of the units are shown in Figs. 4A and 4B. The unit in Fig. 4A has a response map similar to the one in Fig. 3A, with the same general features. The unit in Fig. 4B has an almost entirely inhibitory response map, a pattern of response that is also commonly seen. Figures 4C and 4D show the responses of the same two units to BF tones and to broadband noise (BBN), plotted as discharge rate versus sound level. The BF-tone rate-level functions show the strongly

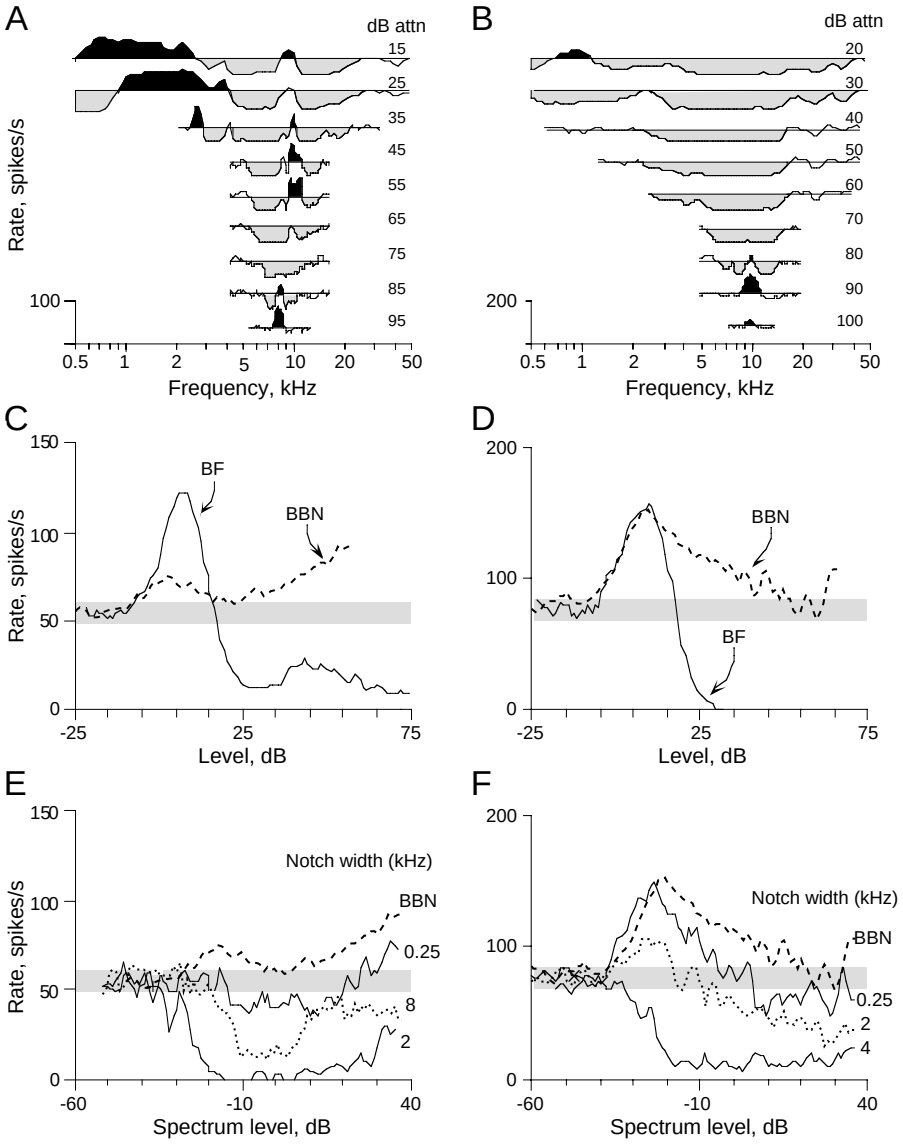

Figure 4. Response maps and responses to broadband noise for two type IV units. Each column shows data from one unit. Response maps are shown in the top row (A and B). Plots of discharge rate versus sound level are shown in the middle row (C and D) for 200 ms BF-tone bursts and noise bursts. The shaded bars show the range of spontaneous rates. For both units, the response to noise is excitatory at all levels, despite the predominantly inhibitory responses to tones. The bottom plots (E and F) show rate-level functions for notch noise, which is broadband noise with a narrow notch or bandstop region centered arithmetically on BF; a sketch of the spectrum is shown in Fig. 7A. The bandwidth of the notch is shown at the right of each curve. Note that the notch responses are inhibitory, which is also not expected from the response maps. Sound levels are given as dB SPL for the BF tones in C and D and as passband dB spectrum level (dB re 20 $\mu Pa/Hz^{1/2}$) in E and F. The BBN rate functions in C and D are aligned at threshold with the BF-tone rate functions, so the abscissa scale is meaningless for them. (Redrawn from Nelken and Young 1994 with permission.)

nonmonotonic shape that is typical of type IV units. Of course, the nonmonotonicity occurs because the tone rate-level function corresponds to moving vertically through the response map at BF, first through the excitatory area near BF threshold and then through the CIA. More important, however, is that the responses to BBN are excitatory at all sound levels, despite the predominantly inhibitory responses to tones. The contrast is clear for the unit in the right column. From the response map, one would predict that the unit's responses to a broadband stimulus should be inhibitory, because inhibitory responses are observed at all frequencies in the response map over a 60 dB range of sound levels. Nevertheless, the net response of the unit to BBN is excitatory. There are clear signs of inhibitory effects in the BBN rate-level functions, in that they are nonmonotonic; nevertheless, the noise responses remain excitatory. This is the typical behavior of type IV units for noise responses.

Figures 4E and 4F show another unexpected characteristic of type IV unit responses to broadband stimuli (Spirou and Young 1991; Nelken and Young 1994); in this case the stimulus is BBN with a notch, or bandstop region, of varying width centered on the unit's BF. The BBN rate-level functions are repeated in Figs. 4E and 4F along with responses to three notch widths. As the notch is widened, the response becomes strongly inhibitory (e.g. the 2 kHz notch width in Fig. 4E and 4 kHz notch width in Fig. 4F). At the widest notch widths, the response becomes less inhibitory, as in the 8 kHz notch width in Fig. 4E, and ultimately becomes excitatory again (not shown; Spirou and Young 1991). The inhibitory response to notches is not expected from the tone response maps by the following argument. The energy that is removed from the noise to make the notch is centered on unit BF; because responses to tone energy near BF is inhibitory in the response map, removing this energy from a BBN should produce an excitatory effect, instead of the inhibitory one that is actually observed. This argument is quite clear for the unit in the right column; it must be made quantitatively for units like the one in the left column because of the small excitatory areas that are present at most levels (Spirou and Young 1991).

The responses of type IV units to broadband stimuli show that these units integrate energy within their response areas in a nonlinear fashion. This point has been demonstrated in several different ways (Nelken and Young 1997; Nelken et al. 1997; Yu and Young 2000). One direct demonstration is to compare tone response maps, like Figs. 3A, 4A, and 4B, with spectro-temporal receptive fields (STRFs) which show the equivalent of a response map constructed from responses to BBN. Whereas tone response maps for type IV units are predominantly inhibitory, the STRFs are predominantly excitatory. In the next section, the nature of the DCN's auditory circuits is analyzed in a way that shows how the nonlinearity of type IV responses arises.

5. The interactions in DCN neural circuits that generate its responses to sound

The nonlinear response characteristics of DCN principal cells can be accounted for by the basic DCN circuit of Fig. 2B. Two inhibitory interneurons are particularly important for responses to sound: the vertical cell, which serves the role of a narrowband inhibitor, and the D-multipolar or radiate neuron of the VCN, which serves the role of a wideband inhibitor. The characteristics of these two inhibitory neurons are shown in Fig. 5, which shows plots of discharge rate versus sound level for BF tones and BBN for a type II unit (Fig. 5A) and an onset-

C unit (Fig. 5B). Type II units are recorded from vertical cells in DCN, as discussed above. Onset-C responses are recorded in the VCN and have been shown to come from multipolar neurons (Smith and Rhode 1989) whose anatomical characteristics are the same as those of the D-multipolar (Oertel et al. 1990) or radiate neurons (Doucet and Ryugo 1997). Most important, these neurons project an axon collateral to the DCN and are glycinergic (Doucet et al. 1999), therefore inhibitory, interneurons. These are the cells marked *W* in Fig. 2.

Type II neurons give a strong excitatory response to BF tones (Fig. 5A) but a weak response to BBN. In this sense, they are a narrowband inhibitor which is active in DCN for stimuli like tones or narrow bands of noise. Natural stimuli, like speech, which have relatively narrow peaks of energy at certain frequencies (the formants in the case of speech) are also likely to activate these units. That type II units inhibit type IV units has been shown using cross-correlation analysis, in experiments where simultaneous recordings were made from a type II and a type IV unit (Voigt and Young 1980, 1990). In appropriate pairs, there is a dip in the discharge probability of the type IV unit immediately after spikes in the type II unit, a so-called inhibitory trough. This is the feature expected of a monosynaptic inhibitory synapse. Inhibitory troughs are seen when the BF of the type II unit is near that of the type IV unit, actually at or just below the type IV BF. This result is consistent with the tonotopic distribution of vertical-cell axons. When a type II and a type IV unit show an inhibitory trough, the excitatory portion of the type II response map usually corresponds well to the CIA of the type IV unit (Young and Voigt 1981), suggesting that the CIA is produced by type II inputs.

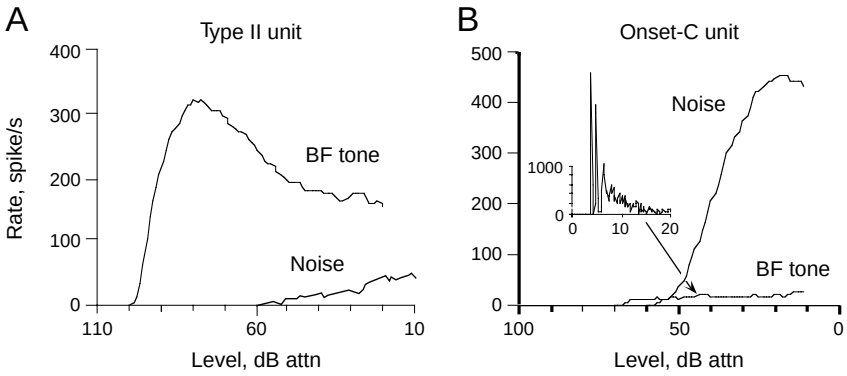

Figure 5. Properties of narrowband and wideband inhibitors in DCN. Discharge rate versus sound level for responses of a type II unit (A) and an onset-C unit (B) to BF tones and broadband noise, as labeled. Rates are calculated from responses to 200 ms tone or noise bursts presented once per second. Sound level is given as dB attenuation. The inset in B shows a PST histogram of this unit's responses to the first 20 ms of 50 ms BF-tone bursts at 45 dB attn.

By contrast, onset-C neurons give weak responses to BF tones and other narrowband stimuli, but strong responses to BBN (Winter and Palmer 1995). This behavior is illustrated by the rate-level functions in Fig. 5B. Palmer and colleagues have characterized the responses of onset-C neurons as resulting from wideband facilitation, meaning that inputs from different frequency ranges interact in a strongly facilitatory way (Winter and Palmer 1995; Palmer et al. 1996). Thus the responses of onset-C neurons increase as bandwidth is widened to a bandwidth well beyond the integrating bandwidth of other CN neurons. The inset in Fig. 5B shows the post-stimulus time (PST) histogram of an onset-C response to BF tones at the sound level indicated by the arrow. The strong onset character of the response and the relatively weak steady state response are evident.

The evidence to associate onset-C neurons with wideband inhibition in DCN is indirect. The primary evidence, discussed above, is that onset-C responses are recorded from a neuron in the VCN that is glycinergic and projects axon collaterals to the DCN (Smith and Rhode 1989; Oertel et al. 1990; Doucet et al. 1999). Onset-C neurons are hypothesized to provide the inhibition to type II neurons that prevents them from responding to BBN (Winter and Palmer 1995) and the inhibition to DCN type IV units that produces inhibitory responses to notch noise (see below; Nelken and Young 1994). In both cases, onset-C neurons have exactly the characteristics needed to produce the inhibition observed in DCN. This is clearest for wideband inhibition of type II units, where the bandwidth of inhibition measured by broadening a band of noise is consistent with the excitatory bandwidth of onset-C neurons, but is wider than the bandwidth of other neurons in the CN (Palmer et al. 1996; Spirou et al. 1999).

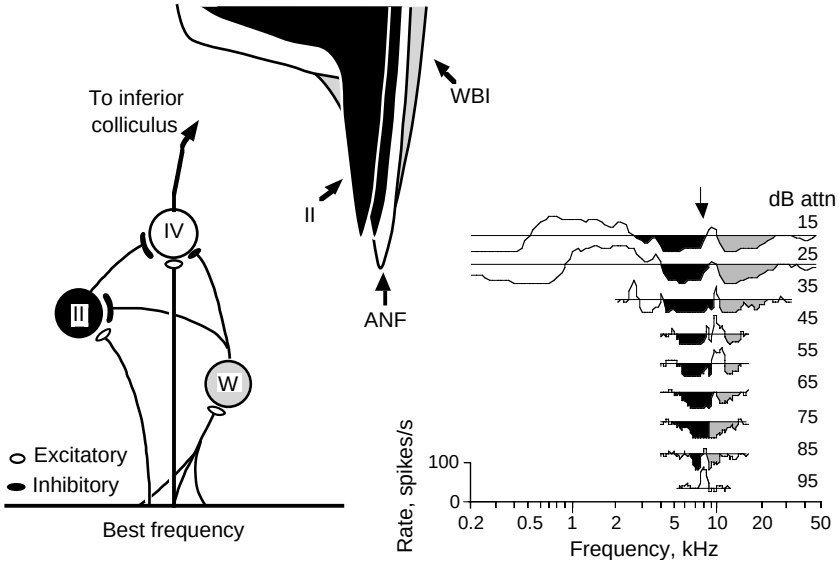

Figure 6. Qualitative model to account for type IV tone response maps. At left is a circuit showing the postulated interconnections of type II and type IV units and the wideband inhibitor (*W*). Excitatory and inhibitory connections are indicated by unfilled and filled ovals, respectively, as shown in the legend. The size of each terminal is an indication of its postulated strength. The horizontal line at bottom represents the tonotopic array of excitatory inputs to the circuit, with BF varying from left to right. The BF of the type IV unit is determined by the BF of its excitatory input; the BF of the type II unit is slightly below that of the type IV. The wideband facilitation of the wideband inhibitor is represented by the broad range of BFs of its inputs. At top center, the outlines of the excitatory areas are shown for the three sources of input to the type IV unit: 1) the excitatory input from auditory nerve fibers (*ANF*) or T-multipolar cells is shown unfilled; 2) the excitatory areas of two type II units are shown in black; and 3) the excitatory tuning curve of a wideband inhibitor is shown shaded. There is probably another inhibitory input with tuning similar to the wideband inhibitor, as is discussed in the next section. At right is a type IV response map with the inhibitory areas shaded, to show the responses contributed by inhibitory inputs in the model.

The tone response map of DCN type IV neurons can be reconstructed qualitatively from the properties of the two inhibitory sources discussed above. The model at left in Fig. 6 shows the interconnections of a type II, a type IV and a wideband inhibitor (simplified from Fig. 2B). The inset at top center of the figure shows the overlapping excitatory receptive fields of the model's three inputs to the type IV unit. The receptive fields are drawn as if they were plotted on standard tuning curve axes of frequency (abscissa) and sound level (ordinate), although the axes are not shown. The white tuning curve marked *ANF* represents the excitatory input to the cell, from auditory nerve fibers and perhaps also from T-multipolars of the VCN. The two black tuning curves represent the excitatory areas of type II neurons. These are aligned with the excitatory tuning curve in a way that is consistent with the data from previous studies. First, the thresholds of the type II units are elevated with respect to the ANF threshold, consistent with the

finding that type II units have higher thresholds than either low-threshold (high spontaneous rate) auditory nerve fibers or type IV units (Young and Brownell 1976; Davis and Young 2000). Second, the type II BFs are shifted somewhat toward frequencies below the ANF BF. This is based on evidence that, in type II-type IV pairs with an inhibitory trough, the BF of the type II unit tends to be below the BF of the type IV unit (Voigt and Young 1990). The type II input is assumed to be strong enough to produce the type IV unit's CIA in the areas of the type II excitatory response. The type IV unit's low-level excitation near BF results from the high thresholds of the type II input; the small excitatory region at the high-frequency edge of the CIA is produced by the slight downward shift of the type II BFs. The type IV's excitatory area at high levels and low frequencies results from the high tail thresholds of the type II units, relative to ANFs (Young and Voigt 1982). The remaining element of the circuit is the wideband inhibitor. The tuning curves of onset-C units tend to have high thresholds and wide bandwidths, consistent with the wideband facilitation model for these cells (Winter and Palmer 1995; Jiang et al. 1996; Palmer et al. 1996). The gray tuning curve shows the hypothesized contribution of the wideband inhibitor to the type IV response map, which is mainly the inhibitory area at frequencies above BF. However, for tones the wideband inhibitor's input is weak, because these units are weakly activated by tones (Fig. 5B) and it is likely that another inhibitory source also contributes to the upper inhibitory sideband (see below; Davis and Young 2000).

The response map at right in Fig. 6 is repeated from Fig. 4A; the inhibitory areas are colored black and gray to show the portions of the map that are hypothesized in the model to derive from the two inhibitory sources. A similar picture could be drawn starting with the response map in Fig. 3A. The response map in Fig. 4B can be produced from the same elements by increasing the bandwidth and strength of the type II inhibitory inputs (Reed and Blum 1995).

Figure 7 shows how the model of Fig. 6 can be used to account for the responses to broadband stimuli shown in Fig. 4. The plots in Figs. 7B, C, and D are sketches of the rate versus sound level functions predicted by the model for narrowband stimuli (tones or narrow noise bands, Fig. 7B), notch noise (Fig. 7C) and broadband noise (Fig. 7D). Figs. 7E and 7F show actual rate-level functions from a type IV unit, for reference. In the model plots, the rate-level functions for the type IV unit and its excitatory input (*ANF*) are plotted in the positive direction and the rate-level functions of the inhibitory inputs are plotted in the negative direction. The assumption used in constructing these plots is that the inputs add to produce the type IV output after weighting by synaptic strengths. For narrowband stimuli (Fig. 7B), the excitatory input (*ANF*) has a monotonic rate-level function typical of both auditory nerve fibers and T-multipolar cells of VCN (Sachs and Abbas 1974; Shofner and Young 1985). The type II unit has a strong response with the characteristically nonmonotonic shape typical of these units (e.g. Fig. 5A). The wideband inhibitor (*WBI*) gives only a weak response, as illustrated in Fig. 5B, and contributes little. Because the type II unit has a higher threshold than the excitatory input, the type IV unit is excited at low sound levels, but then is inhibited when the type II unit begins to fire. The correspondence of the type II excitatory threshold and the type IV inhibitory threshold, meaning the sound level at which the type IV rate reaches a peak and begins to decline, has been demonstrated for type II-type IV pairs that show an inhibitory trough (Young and Voigt 1981) and also in the population of type II and type IV units (Davis and Young 2000). The type II inhibitory input is strong enough to inhibit the discharge of the type IV unit at high sound levels,

resulting in the CIA and the characteristic non-monotonicity of type IV units for narrowband stimuli centered near BF (Figs. 4C, 4D, and 7E).

For broadband noise (Fig. 7D), the excitatory input behaves approximately the same as for tones. The wideband inhibitor gives a strong response in this case. Because of the inhibition from the wideband inhibitor, the type II unit gives a weak response and contributes little to the type IV response. The type IV response is the resultant of the excitatory input minus the inhibition from the wideband inhibitor. The strength of the inhibitory synapse from the wideband inhibitor is presumed to be relatively weak, so that it produces only partial inhibition of the type IV unit, giving the weak excitatory response typical of type IV units for broadband noise (Figs. 4C, 4D, and 7F).

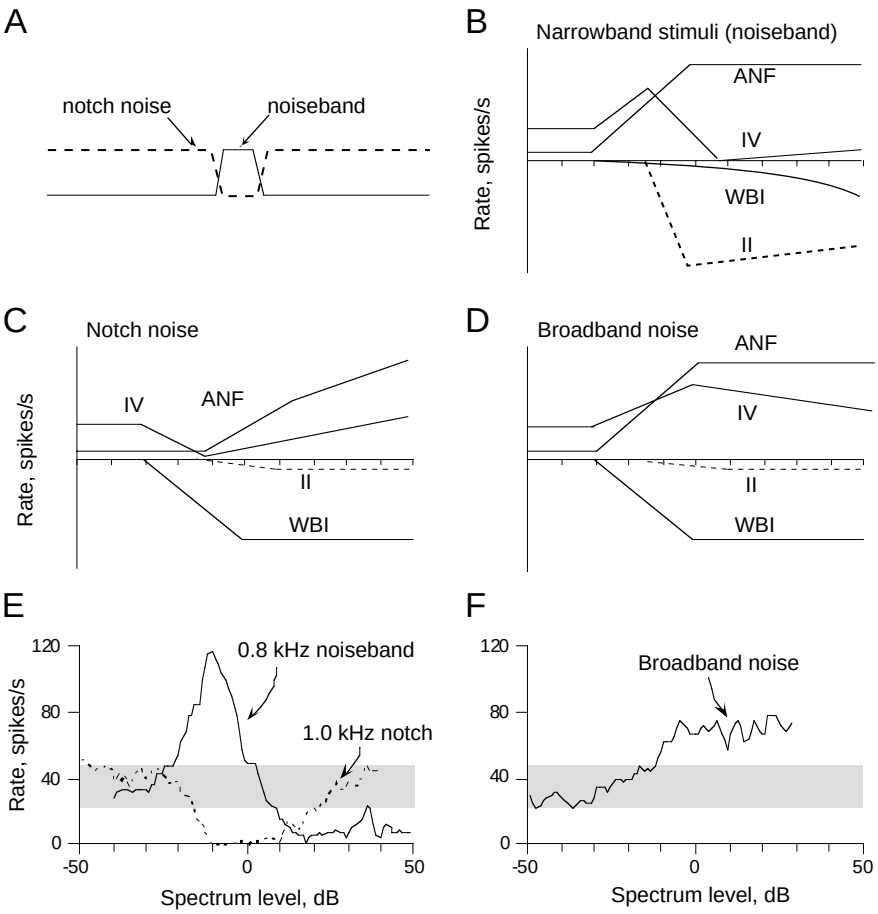

Figure 7. Qualitative explanation of the rate-level functions of type IV neurons and their derivation from inputs, using the model of Fig. 6. A. Spectra of a noiseband and a notch noise. In all cases, the noise band or the notch are centered on the type IV BF. B, C, and D. Sketches of rate-level functions for a type IV unit (*IV*, heavy line), its excitatory input (*ANF*), and two sources of inhibitory input (type II, dashed line, and the wideband inhibitor, *WBI*). The excitatory input is shown positive and the inhibitory inputs are negative. The rate-level functions have approximately correct relative amplitudes and thresholds, according to data. The spontaneous rate of the type IV unit is assumed to be partly intrinsic and partly due to spontaneous activity in the excitatory inputs. The synapse strengths are fixed in B, C, and D and are constrained in the following ways: the type II synapse must be strong enough to overcome the excitatory input in B and produce partial or complete inhibition of the type IV unit for narrowband stimuli; the WBI synapse on the type IV must be weak enough to produce only partial inhibition of the type IV unit for broadband noise in D, but still strong enough to produce inhibition with the weakened excitatory input in C; and the WBI synapse on the type II unit must be strong enough to produce near-zero rate in the type II for both broadband noise and notch noise. E and F show examples of noiseband, notch noise, and broadband noise responses from a type IV unit. (E and F redrawn from Nelken and Young 1994 with permission.)

Finally, with notch noise, the situation is similar to the case of broadband noise, in that the wideband inhibitor is strongly activated and the type II unit is not (Fig. 7C). Activation of the wideband inhibitor occurs because these neurons receive and integrate excitatory inputs across a relatively broad array of BFs, the broadband facilitation mentioned above. For notch widths that

are narrower than the bandwidth of the wideband inhibitor's excitatory inputs, it will still receive enough input to be activated. By contrast, the excitatory input to the type IV unit is narrowband; the energy removed to make the notch reduces substantially the excitatory input. The effect is a shift in threshold and a decrease in the slope of the ANF rate function (Schalk and Sachs 1980; Poon and Brugge 1993). The type II response is also weak, both because the wideband inhibitor is activated and because of reduced excitatory input near BF. As a result, the wideband inhibitor is the strongest input to the type IV unit for notch noise and the net response of the type IV unit is inhibitory (Figs. 4E, 4F, and 7E). Type IV units show a range of sensitivities to notch width (Nelken and Young 1994). The net effect of a particular notch width on a type IV unit presumably depends on the relative integrating bandwidths of the excitatory and wideband inhibitor inputs. As long as more energy is removed from the excitatory than from the inhibitory inputs, the type IV response will be inhibitory. The qualitative model shown in Figs. 6 and 7 has been quantified to show that it can successfully account for most properties of type IV neurons in DCN (Blum et al. 1995; Hancock et al. 1997; Blum and Reed 1998).

According to the model, the nonlinearity of DCN principal cell responses results from the fact that the DCN circuit switches from one dominated by type II units for narrowband stimuli to one dominated by the wideband inhibitor for broadband stimuli. Because neither inhibitor is spontaneously active, the switch behaves like a rectifier, producing nonlinear responses. For example, the lack of spontaneous activity in type II units means that a broadband stimulus produces no effect through the type II circuit; if type II units were spontaneously active, the inhibition of type II units by broadband stimuli through the wideband inhibitor would appear as disinhibition in type IV neurons. The result would be a smooth transition from inhibitory to disinhibitory effects in type IV units as the bandwidth widens, instead of a sudden disappearance of the type II unit at zero rate. In fact, many of the nonlinearities in DCN principal cell responses occur at the point where type II units reach threshold (Nelken and Young 1997).

6. Inhibitory and excitatory inputs to principal cells from the superficial DCN and the effects of somatosensory inputs

The model presented in the previous sections does not include the effects of the neuropil in the superficial DCN. As described in Fig. 2, DCN pyramidal cells receive excitatory inputs from the parallel fibers of the molecular layer and inhibitory inputs from interneurons located there. Giant cells in deep DCN do not have extensive dendritic trees in the molecular layer; however, on physiological grounds, they receive inputs from at least a part of the circuitry of the superficial layer (Davis et al. 1996b; Golding and Oertel 1997). Figure 8 shows typical effects of electrical stimulation of the somatosensory inputs to the DCN from the MSN; data are shown for type IV (Figs. 8A,B), type II (Fig. 8C), and complex-spiking units (Fig. 8D). For each plot, the top trace shows the extracellular evoked potential (EP) at the DCN recording site. The stimulus was a sequence of four shocks delivered to the MSN at the times of the arrows at the top of the figure. The evoked potentials serve as a marker of the synaptic currents produced in the molecular layer by activation of the parallel fibers (Young et al. 1995). The bottom traces are PST histograms of the responses to the stimulation for DCN units that were otherwise firing spontaneously, except for the type II unit in Fig. 8C which was activated by a BF tone 10 dB

above threshold. The response of the type IV unit in Fig. 8A shows three components: 1) a short-latency inhibitory component that precedes the onset of the EP (marked by the dashed lines); 2) a transient excitatory component (bold) just after the onset of the EP; and 3) a long-latency inhibitory component which follows the excitatory component. Approximately half of all type IV units show this response pattern to MSN stimulation, while most of the remainder show only the third long-latency inhibitory component, as for the unit in Fig. 8B. Note that the long-latency inhibitory component begins after the onset of the evoked potential in Fig. 8B. Although the source of the short-latency inhibition is unknown, the excitatory component likely reflects direct excitation of principal cells by parallel fibers (Manis 1989; Waller et al. 1996) and the long-latency inhibition is probably produced by input from cartwheel cells (see below; Davis and Young 1997). Type II inhibitory inputs to DCN principal cells are themselves weakly inhibited by MSN stimulation (Fig. 8C; Young et al. 1995); onset C neurons are weakly excited by MSN stimulation, but only in the presence of an acoustic stimulus (K.A. Davis unpublished). Thus the long latency inhibition of type IV units cannot be produced by excitation of either type II or onset-C inhibitory circuits.

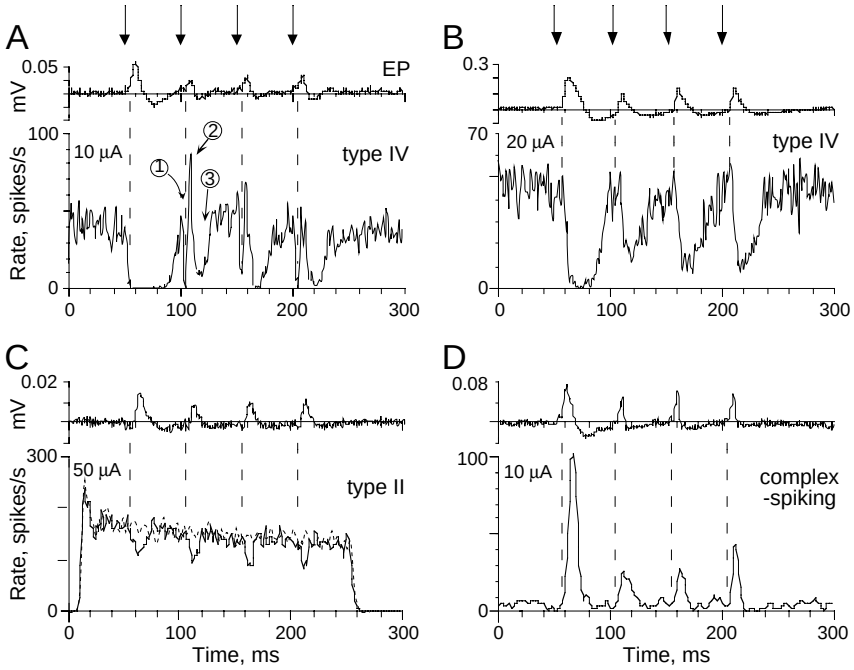

Figure 8: Responses of two DCN type IV units (A and B), a type II unit (C), and a complex-spiking unit (D) to electrical stimulation in the MSN. Arrows at the *top* show the times of the 4 electrical pulses, which were spaced 50 ms apart and presented once per second; the current level is given above the histograms. In C, a 250 ms tone at BF, 10 dB above threshold, was presented to produce background activity (dashed line); the solid line shows the responses to the electrical stimulus in the presence of the tone. For each panel, the *top plot* shows the evoked potential (EP) at the recording site and the *bottom plot* shows a PST histogram of the responses. Vertical dashed lines are aligned with the onsets of the EPs at the DCN recording site. The three components of the type IV response in A are numbered to correspond to the discussion in the text. The type IV unit in B shows only the third long-latency component. The type II unit in C shows only weak long-latency inhibition. The complex-spiking unit in D shows an excitatory response that corresponds in latency and adaptation properties to the long latency components in A and B. Histograms were constructed from 400 repetitions of the stimulus using a binwidth of 1 ms. In all cases, the electrical stimulus was applied at a site in the MSN somatotopic map where the pinna was represented. (A and B redrawn from Davis et al. 1996b and D redrawn from Davis and Young 2000 with permission.)

Evidence that cartwheel cells are the source of the long-latency inhibitory component is shown in Fig. 8D. In contrast to type IV units, complex-spiking units are strongly excited by MSN stimulation. This excitatory response coincides in time with the onset of the EP (dashed lines) and shows a characteristic adaptation pattern: strongest at the first pulse, weakest at the

second pulse, and then increasing in strength at subsequent pulses. Comparison of Figs. 8B and 8D shows that the latency and four-pulse amplitudes of the complex-spiking unit responses correspond exactly to the long-latency inhibitory responses of type IV units, suggesting that cartwheel cells are the source of this component. These comparisons are made in more detail elsewhere (Davis and Young 1997).

Somatosensory inputs to DCN can be activated by stimulating many parts of the body (Saadé et al. 1989; Young et al. 1995), but by far the strongest effects are from the pinna. The EPs in DCN are largest when electrical stimulation is applied to the pinna representation of the somatosensory map in the MSN (Young et al. 1995) and are also largest when spinal nerve C2 is stimulated (Kanold and Young 1998). C2 is the nerve that carries sensory fibers from both the skin and muscles associated with the pinna (Hekmatpanah 1961; Abrahams et al. 1984a,b). The modality of the somatosensory effects in DCN is clearly muscle sense, not skin sense (Kanold and Young 1996, 1998). That is, touching the skin or hairs on the pinna and surrounding skin rarely causes any effect in DCN. Instead the effective stimuli are actions that stretch the muscles that move the pinna. Both lateral extension of the pinna and vibration applied to the pinna muscles are strong stimuli; both actions should primarily stimulate muscle stretch receptors and tendon organs. Thus the somatosensory inputs to the DCN seem to convey information about the contractile state of the muscles that move the pinna, and therefore about the orientation of the pinna. The circuitry in the superficial DCN conveys this information to the DCN principal cells, where it is integrated with auditory information from the circuitry in the deeper layers.

7. Evidence for DCN circuits from pharmacological manipulations

The three inhibitory circuits described above, i.e. the vertical, radiate, and cartwheel cells, are all glycinergic (Oertel and Wickesberg 1993; Golding and Oertel 1997; Doucet et al. 1999). A test of the model described in the previous section is to apply pharmacological antagonists to glycine and γ-aminobutyric acid (GABA), the other common inhibitory neurotransmitter, and examine whether responses change in the expected way. Figure 9 shows the effects on DCN responses of iontophoretic application of strychnine, a glycinergic antagonist, and bicuculline, a GABAergic antagonist. The antagonists were applied to the recording site of the neurons from a pipette glued to the recording electrode (Davis and Young 2000). This figure shows that strychnine has the effects expected from the model (see also Caspary et al. 1987; Evans and Zhao 1993). Figure 9A shows BF rate-level functions for a type IV unit before, during, and after iontophoretic application of strychnine and bicuculline. Under control conditions (thin solid line), the type IV unit had a nonmonotonic rate-level function, typical of type IV units. In the presence of strychnine (heavy line), the unit lost entirely its inhibitory responses to high-level tones, with the result that the function became monotonic; there was also an increase in the spontaneous discharge rate (dark gray band). Figure 9C shows that strychnine similarly releases type IV unit responses to broadband noise. Here, the unit showed a weak excitatory nonmonotonic rate-level function to noise in control conditions (thin solid line) and a strong, monotonic response during strychnine application (heavy line); again, there was an increase in spontaneous activity.

The strychnine data can be interpreted as follows: Fig. 9A shows release of inhibition produced primarily by vertical cells, which are the most active inhibitory interneuron during presentation of tones; Fig. 9C shows release of inhibition produced primarily by the wideband inhibitor, which is most active during presentation of noise. Increases in spontaneous rate were observed in about half the cases (Davis and Young 2000). Because neither vertical cells nor wideband inhibitors are spontaneously active, changes in spontaneous rate must reflect inhibition from other, as yet unidentified, sources. Not shown in Fig. 9 is that strychnine also blocks both the short- and long-latency inhibition produced by MSN stimulation in type IV units (Davis and Young 2000). In the case of the long-latency inhibition, the strychnine effect presumably acts by blocking inhibition from cartwheel cells.

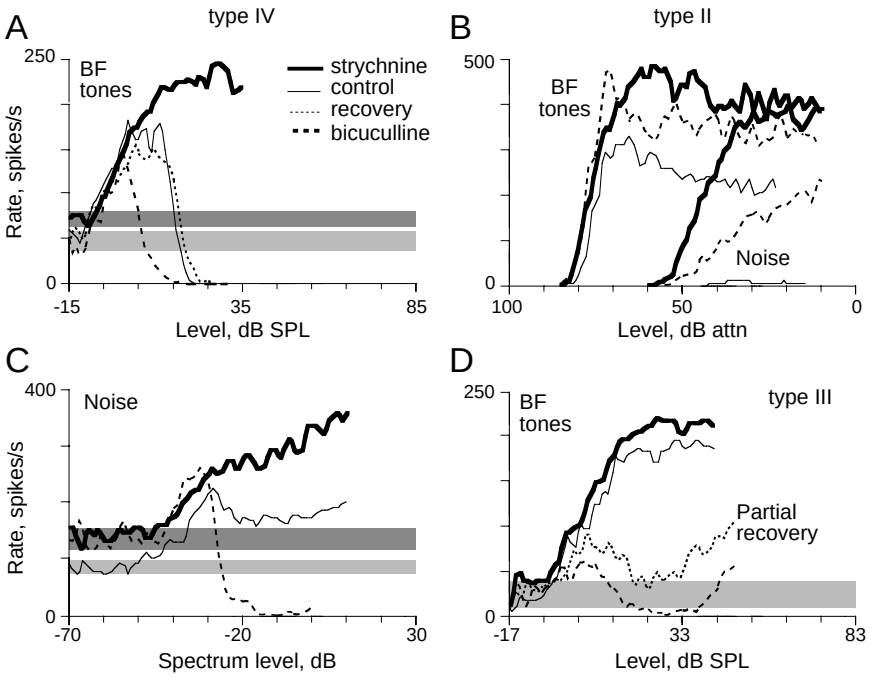

Figure 9. Comparison of the effects of strychnine and bicuculline on the BF-tone and noise rate-level functions of DCN type IV, type II, and type III units. The line weight identifies the conditions, as described in the legend. Thin solid lines show responses before application of any agent and thin dotted lines show recovery data. The recovery curves in A and D are after bicuculline but before strychnine application. The shaded bars show the range of spontaneous discharge rates before (light shading) and during (heavy shading) application of a drug (strychnine in A; strychnine and bicuculline in C). The stimulus (BF-tone or noise) is given at left in each panel, except in B where stimulus type is identified next to the curves. Note that strychnine abolished the inhibitory responses of the type IV unit at BF (A) or in response to noise (C), whereas bicuculline enhanced inhibitory responses (i.e. units were inhibited at lower sound levels and more strongly). In contrast, both drugs increased the discharge rate of the type II unit (B) and lowered the excitatory threshold slightly. Bicuculline converted the type III unit into a type IV unit (D). (A, C, and D redrawn from Davis and Young 2000 and B redrawn from Spirou et al. 1999 with permission.)

Although GABAergic neurons are not part of the model described above, there are many GABAergic cells in the CN, especially in the superficial DCN (Mugnaini 1985; Roberts and Ribak 1987; Osen et al. 1990). Golgi cells in the granule cell areas, including those in the DCN, and small cells scattered throughout the CN are GABAergic. Cartwheel cells colocalize GABA and glycine, although they seem to be functionally glycinergic (Golding and Oertel 1997; Davis and Young 2000). In addition, there are GABAergic efferent projections to the CN from other parts of the auditory system (Ostapoff et al. 1990, 1997). Although the responses to sound of these GABAergic systems are not known, some properties of a GABAergic inhibitory system can be inferred from the effects of GABA antagonists on DCN responses. Figure 9 shows that

application of the GABA-A antagonist bicuculline has unexpected effects on DCN principal cells. The heavy dashed line in Fig. 9A shows that bicuculline did not abolish the inhibition produced by BF tones; instead, the inhibition was stronger in the presence of bicuculline, in that the inhibitory threshold was lower. A similar result is shown for noise-driven responses in Fig. 9C. The noise rate-level function became strongly nonmonotonic with bicuculline, demonstrating stronger inhibition (heavy dashed line).

The effects of both strychnine and bicuculline on type II units are what one expects for inhibitory antagonists. Figure 9B shows BF-tone and noise rate-level functions for a type II unit under control conditions and during iontophoretic application of strychnine and bicuculline. Under control conditions (thin solid lines), the type II unit had no spontaneous activity, gave excitatory responses to BF tones at all sound levels, and responded with a rate near zero to broadband noise. While neither drug alone or in combination endowed the unit with spontaneous activity, both strychnine (heavy solid line) and bicuculline (heavy dashed line) produced substantial increases in response to both tones and noise. Both drugs also reduced the threshold slightly. The effects of strychnine on type II units are consistent with the hypothesized strong inhibitory input to these neurons from the wideband inhibitor. The effects of bicuculline imply that there is an additional strong GABAergic input to type II neurons. The source of the GABAergic input is not known.

The most dramatic bicuculline effects occur in type III units, illustrated in Fig. 9D. In control conditions, type III units show monotonic or near-monotonic rate-level functions to BF tones (thin solid line). Bicuculline converted this type III rate function into a nonmonotonic curve resembling a type IV unit (heavy dashed line). While the unit was still recovering from the bicuculline (dotted line marked partial recovery), strychnine was applied, resulting in abolition of the inhibition and a monotonic rate-level curve (heavy solid line). This result suggests that the bicuculline-enhanced inhibition in type III units is mediated by a glycinergic interneuron. Given that the stimulus was a BF tone, the glycinergic interneuron was most likely a type II unit.

The effects of bicuculline on type III and IV units in Fig. 9 can be explained by assuming that the iontophoresed drug is spreading from the recording site of the principal cell to nearby type II neurons. Type II neurons often can be recorded on the same microelectrode with type III and type IV neurons (Voigt and Young 1980), which implies that their cell bodies are close together. Moreover, the strongest inhibitory cross-correlation is observed for type II/type IV pairs that are close together (Voigt and Young 1990). Thus it is reasonable to suppose that the substantial release from inhibition observed in type II units when bicuculline is applied (Fig. 9B) occurs also when bicuculline is iontophoresed near a type III or type IV unit. The changes in type III and IV response seen in Fig. 9 are then explained as a secondary consequence of release from inhibition in type II neurons, with the additional assumption that there are few GABAergic synapses on principal cells, or that those synapses are weak. Consistent with this suggestion, the bicuculline-induced changes of the tone thresholds in type II units are in the same direction as and similar in amplitude to the changes in inhibitory thresholds in type IV units (-4 dB versus –3 dB; Davis and Young 2000).

Bicuculline has little or no effect on the inhibition of type IV units by electrical stimulation of the MSN, either short- or long-latency (Davis and Young 2000), supporting the conclusion that the cartwheel-cell inputs to principal cells are glycinergic and suggesting that the

unknown short-latency inhibitor is also glycinergic. However, the responses of cartwheel cells to MSN stimulation are increased following bicuculline application at their recording sites. Thus the cartwheel cells must receive direct or indirect GABAergic inhibition activated by the mossy fiber inputs to DCN. A likely substrate for this inhibition is the Golgi cell, which could inhibit both granule cells and cartwheel cells.

The discussion above is based on the effects of antagonists at BF only; off-BF responses show new features which demonstrate the presence of an additional inhibitory input to type IV neurons. Figure 10 shows the effects of strychnine and bicuculline on the response maps of two type IV units. Neither drug alone can eliminate all the inhibition present in type IV response maps. The top half of Fig. 10 shows a type IV response map in control conditions (Fig. 10A) and during strychnine application (Fig. 10B). The vertical line in Fig. 10A is aligned with the excitatory edge of the CIA and separates this unit's inhibitory response into its CIA and an upper inhibitory sideband. In the presence of strychnine (Fig. 10B), the CIA is eliminated and replaced with excitation, consistent with the model and previous results (Figs 9A). The inhibition above BF, however, is reduced but not eliminated by strychnine. The residual inhibition in these response maps is likely to be GABAergic in origin, as is illustrated by the second example in Fig. 10.

The bottom half of Fig. 10 compares the response map of another type IV unit in control conditions (Fig. 10C) and with bicuculline (Fig. 10D). The bicuculline enhanced the CIA, which is most clearly seen at 70 dB where the near-BF excitatory response was abolished. However, the opposite effect is observed for frequencies away from BF; the upper inhibitory sideband was converted to excitation and a weak

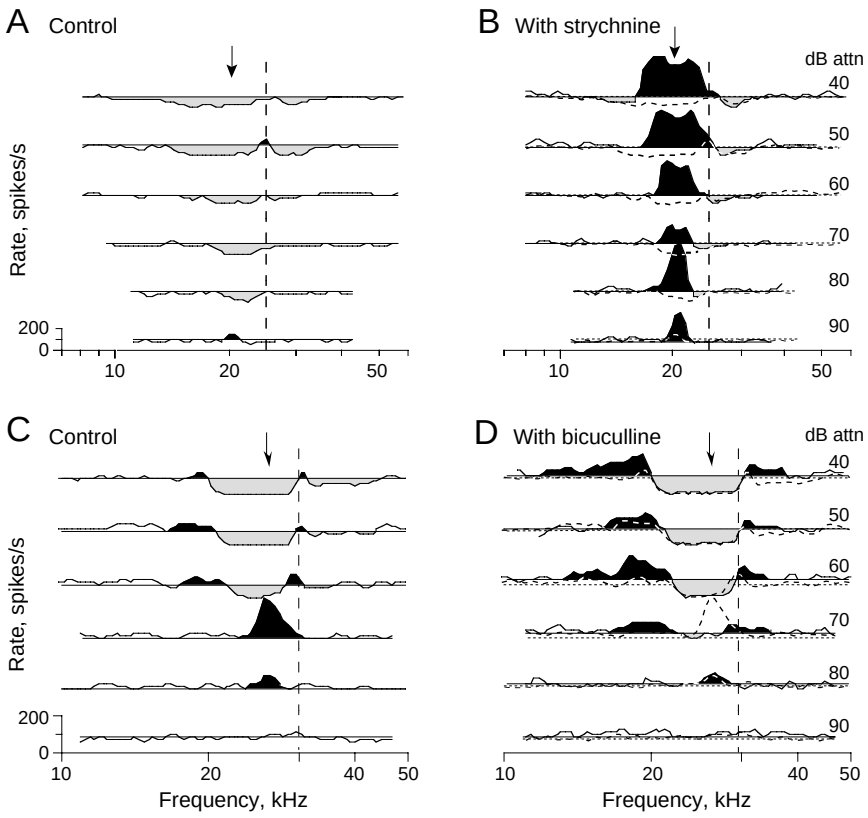

Figure 10. Frequency response maps of DCN type IV units before (left) and during (right) iontophoretic application of strychnine (top) or bicuculline (bottom). The control response maps are repeated in the right column with dashed lines to allow comparison. The vertical lines separate the CIA to the left of the line from the upper inhibitory sideband to the right. The arrows at top point to BF. A and B show the effects of strychnine on one unit. In B, strychnine abolished most of the CIA and reduced, but did not eliminate, the upper inhibitory sideband. C and D show the effects of bicuculline on a different neuron. Note the enhancement of the CIA near BF (e.g. the response at 70 dB attenuation), but the weakening of inhibition or enhancement of excitation away from BF (at levels from 40-70 dB attenuation). (Redrawn from Davis and Young 2000 with permission.)

excitatory response below BF was enhanced by the bicuculline. These results suggest that there is an additional inhibitory input to principal cells which is GABAergic. It is apparently weaker than the type II glycinergic inhibition that produces the CIA, so it is only clearly seen at frequencies outside the CIA. The upper inhibitory sideband in type IV units is apparently due to two effects: this GABAergic inhibitor and the glycinergic wideband inhibitor as in Fig. 6. The GABAergic effect appears to be stronger for tones away from BF (compare Fig. 10D with Fig. 10B), but the glycinergic effect dominates in broadband noise (Fig. 9C).

8. Circuit model of the DCN

The results of this and the previous section imply that the circuit model of Fig. 6 is incomplete with regard to the synaptic inputs of DCN neurons. At least two additional elements must be added, the cartwheel cells of the superficial DCN and at least one GABAergic source, of unknown origin. Figure 11 shows a modified circuit model that includes these two elements, as well as a granule cell of the superficial layer. The cartwheel cells synapse on type IV neurons, and weakly or not at all on the type II and WBI interneurons (e.g. those neurons give little or no inhibitory response to MSN stimulation, Fig 8C and Young et al. 1995). The GABAergic source must be activated by both somatosensory and auditory inputs in order to explain the results summarized in the previous section and terminates on type II, type IV, and cartwheel cells. Its effects are strongest on the cartwheel and type II neurons and are relatively weak on principal neurons. It is not clear that there is only one GABAergic source, but only one is shown in Fig. 11 for parsimony. Evidence that there is more than one is provided by the fact that bicuculline iontophoresis at type IV recording sites affects these cells' responses to off-BF tones, but not to MSN stimulation. This result seems to require two GABAergic sources, one more strongly driven by sound and one more strongly driven by the granule cell circuits.

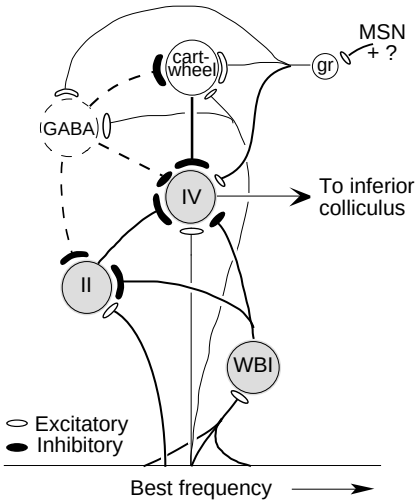

Figure 11. Circuit model of the DCN that includes all the effects described above. Shaded neurons are the primarily auditory neurons described in Fig. 6. The granule cell and cartwheel cell of the superficial layer and a GABAergic neuron of unknown identity have been added. The relative size of synaptic terminals corresponds roughly to the relative synaptic strength needed to account for the effects described above. (Redrawn from Davis and Young 2000 with permission.)

One role of the GABAergic neuron is apparently to regulate the strength of type II inhibition in DCN. Type III and type IV neurons can be understood as forming a continuum of principal cell responses, in which type IV neurons are seen when the GABAergic inhibition of type II neurons is weak and type III neurons are seen with strong GABAergic inhibition. This hypothesis is consistent with the effects of pentobarbital anesthesia on the DCN. In anesthetized animals, type IV units are rare and, in decerebrate preparations, type IV units are converted to type III when pentobarbital is given intravenously (Evans and Nelson 1973; Young and Brownell 1976). Because one effect of pentobarbital is to potentiate GABAergic inhibition (e.g. Richter and Holtman 1982), type II

units would be more strongly inhibited by their GABAergic inputs in anesthetized animals, which should bias the principal cells toward type III. Another possibility is that the level of GABAergic tone in an animal could account for the difference in prevalence of type III versus type IV neurons between species. In decerebrate cat, type IV units predominate (57% of principal cells; Shofner and Young 1985), whereas in decerebrate gerbil, type III units predominate (85%, Davis et al. 1996a).

9. Responses of DCN neurons to acoustic cues for sound localization

The evidence discussed at the beginning of this chapter suggests that the DCN is involved in integrating information about sound localization. Both behavioral results (Sutherland et al. 1998b; May 2000) and the fact that the DCN receives somatosensory inputs that carry information about the position of the pinna (Kanold and Young 1996) support this idea. Given this hypothesis, it is interesting to ask how DCN principal cells respond to the acoustic cues that convey information about sound location. Sound localization cues are both binaural and monaural. The DCN is primarily a monaural nucleus, although it does receive inputs from the contralateral ear (Mast 1970; Young and Brownell 1976). However, the contralateral inputs are weak and do not produce sensitive responses to either interaural time differences or interaural level differences. Certainly the binaural responses in DCN are insensitive in comparison to the binaural responses of cells in the superior olive and inferior colliculus. In contrast, DCN type IV units are particularly sensitive to monaural cues, that is, to spectral sound localization cues of the kind produced by the cat external ear (Young et al. 1992, 1997). This sensitivity has been shown to give DCN principal cells a sensitivity to the direction of a sound source (Imig et al. 2000).

Figure 12 shows an example of the responses of a type IV unit to spectral cues. The stimulus used in this experiment was broadband noise filtered by the HRTF (Fig. 1) from one direction in space; thus the power spectrum of the noise was equal to the magnitude spectrum of a HRTF filter. This situation simulates presentation of a broadband noise in free field from a speaker located in the direction of the HRTF. The strongest response produced by DCN type IV units to HRTF-filtered stimuli is an inhibitory response when a spectral notch is centered on BF. Figure 12B shows the response map of a DCN type IV unit and Fig. 12A shows part of the power spectrum of a HRTF-filtered noise on the same frequency scale. The power spectrum is repeated three times, labeled *a*, *c*, and *e*. These three spectra are from one stimulus that was presented at three different sampling rates of the D/A converter used to generate the stimuli; this manipulation has the effect of shifting the spectrum to the left or right along the (logarithmic) frequency scale. The unit's sensitivity to particular features in the stimulus spectrum can be investigated by studying the responses with those features located at various frequencies relative to BF. Figures 12C and 12D show discharge rate versus sound level for the HRTF stimulus with its sampling rate adjusted to place the notch at five different frequencies, labeled *a* through *e* in Fig. 12B. When the notch was centered on BF (*c*), the response was strongly inhibitory across almost the entire range of sound levels. As the notch was moved away from BF, the inhibitory response disappeared and was replaced by an excitatory response reminiscent of this unit's response to broadband noise. At positions *a* and *e* the notch center was only –0.19 and 0.14 octaves away from BF; nevertheless the response to the notch had disappeared, showing that this

unit had a very sensitive response to the position of a notch relative to BF. As discussed above, this response cannot be understood from the response map, but is accounted for by the circuit model of Figs. 6 and 7.

The inhibitory response to spectral notches shown in Figs. 12C and 12D is a property only of DCN principal cells. Neurons in VCN show no sign of the inhibitory response and even DCN cells vary considerably in their sensitivity to the notch. This behavior is illustrated by the data in Fig. 13. Figures 13A-C show plots of rate versus sound level for HRTF-filtered stimuli. In each case the sampling rate was adjusted to place a notch at BF (labeled *B*), just below BF (*U*), or just above BF (*L*). When the notch was below or above BF, the sampling rate was chosen to place the BF just at the shoulder of the notch, as in cases *a* and *e* in Fig. 12 (*U* means the BF is at the upper shoulder of the notch and *L* refers to the lower shoulder). In most units, when the notch is below or above BF, the response resembles the unit's response to broadband noise, as in Fig. 12. It is the response to the notch at BF that varies most among units. The case in Fig. 13A is like the case in Fig. 12 in that the response is strongly inhibitory at BF. This

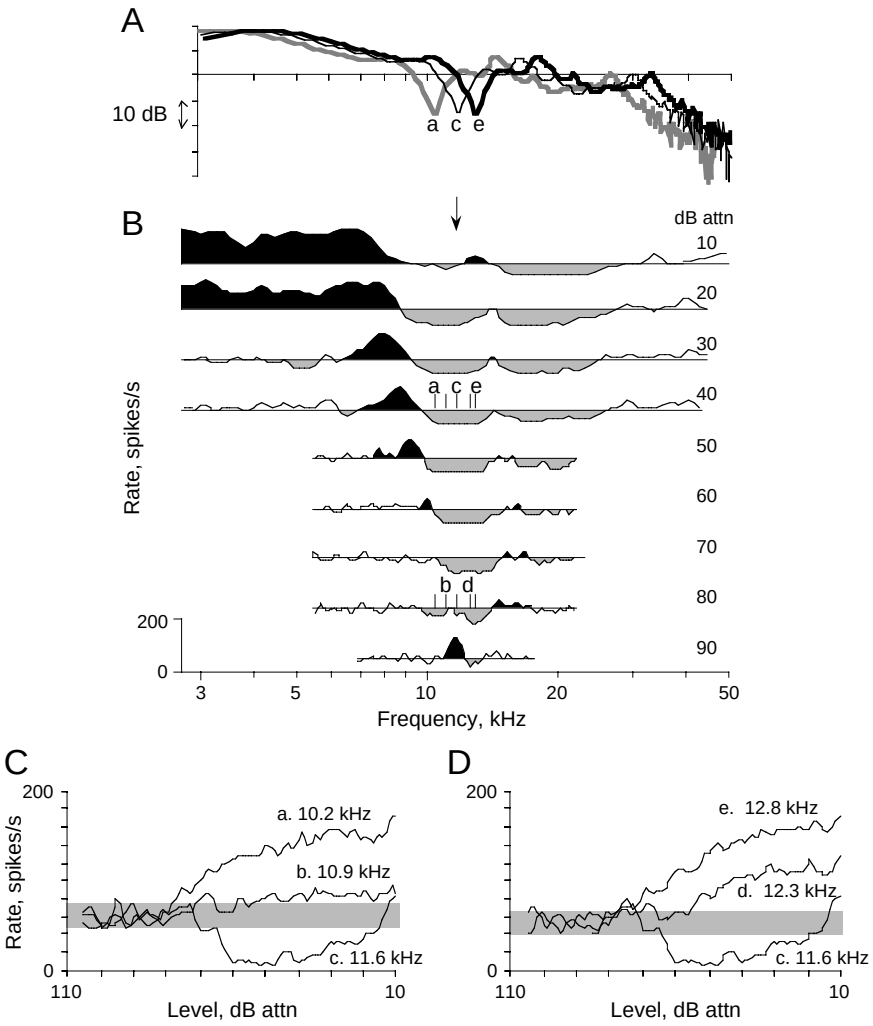

Figure 12. A. Power spectra of broadband noise filtered with a HRTF spectrum and presented as a stimulus to the type IV unit shown below. The sampling rate of the D/A converter used to generate the stimuli was varied in order to shift the stimulus spectrum along the frequency axis. The positions of the center of the prominent spectral notch for five sampling rates are labeled *a* through *e* in this figure. Three of the spectra are plotted in A. B. Response map of a type IV unit. The positions of the centers of the notches are marked with vertical ticks on the 40 dB and 80 dB lines of the map. The notch was at BF for stimulus *c*. C. D. Plots of discharge rate versus sound level for the HRTF filtered stimuli at the five sampling rates; rates are for responses to 200 ms bursts of noise presented once per second. The labels on each curve identify the notch center frequencies with the actual frequencies and the labels *a* through *e*. Notice the strong inhibitory response when the notch is at BF (*c*) which is replaced by an excitatory response as the notch moves away from BF in either direction. (Redrawn from Young et al. 1997 with permission.)

inhibitory response is seen only in type III and type IV units in DCN. The unit in Fig. 13C shows responses typical of VCN neurons and auditory nerve fibers (Poon and Brugge 1993), and also some DCN neurons. There is only a shift in the rate function to higher sound levels when the notch is at BF. In the VCN and the auditory nerve, the shift in the rate function is presumably due to the reduction in stimulus power within the unit's tuning curve when the notch is located at BF. In addition there is sometimes a reduction in the saturation rate with the notch at BF; this reduction reflects inhibition in the VCN or cochlear two-tone suppression. The case in Fig. 13B is intermediate between the other two examples; this type IV unit shows a reduction of rate to near zero when the notch is located at BF. From the model of type IV units and the explanation in Fig. 7C, it seems likely that the differences among the type IV units in Figs. 13A and 13B can be explained by differences in the excitatory and inhibitory integrating bandwidths of the neurons' inputs, as discussed previously, or by differences in the synaptic strength of the wideband inhibitor.

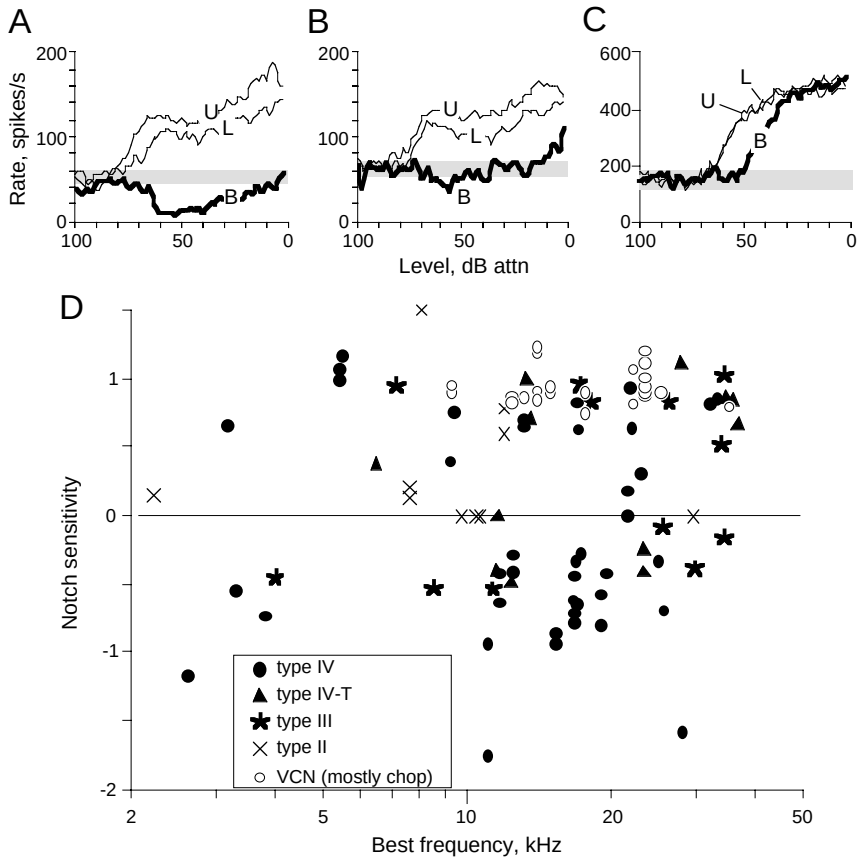

Figure 13. A, B, C. Discharge rate versus sound level for HRTF-filtered noise stimuli with spectra like those in Figs. 1A, 1B, and 12A. The HRTFs used have been shown elsewhere (Fig. 1 in Rice et al. 1995). The sampling rate of the D/A converter used to produce the stimulus was adjusted to place a notch at BF (*B*) or so that the BF was at the upper (*U*) or lower (*L*) shoulder of the notch, as illustrated by positions *c*, *a*, and *e* respectively in Fig. 12B. Sound level is given as attenuation, but the spectrum level of the stimulus was the same for the three curves in each plot. Rates are computed from 200 ms stimuli presented once per second; shaded bars show spontaneous discharge rates. Units in A and B are DCN type IV, unit in C is from VCN. D. Scatter plot of notch sensitivity versus BF for a population of DCN and VCN neurons. Notch sensitivity is the ratio of the saturation rate, re spontaneous rate, of responses with the notch at BF (*B* in parts A-C) to the average saturation rate, re spontaneous, of the responses with the notch above or below BF (*L* and *U*). The saturation rates were taken as the maximum or minimum rate near the first inflection point in the rate plot (e.g. at –60 dB, -68 dB, and –56 dB for *B*, *U*, and *L* respectively in A). The notch sensitivity is –0.6 for the data in A, -0.3 for the data in B, and +1 for the data in C. Neuron types are identified by symbols, defined in the legend. VCN

Figure 13D shows a summary of the notch responses of DCN and VCN neurons. The ordinate of this plot is an index of notch sensitivity equal to the ratio of the saturation rate with the notch at BF (rate minus spontaneous rate) divided by the average saturation rate with the

notch above and below BF (also rate minus spontaneous rate). Units like Fig. 13A have negative notch sensitivity values, units like Fig. 13B have notch sensitivities near 0, and units like Fig. 13C have notch sensitivities near +1. Thus the notch sensitivity is an index of the presence of the inhibitory response with the notch at BF. In Fig. 13D, notch sensitivity is plotted versus the units' BFs. Symbols identify the different unit types, as defined in the legend. Units from VCN (unfilled circles) all show notch sensitivities near +1 (median of 0.92). These units are not inhibited or only weakly inhibited by the notch at BF. DCN type II units (Xs) have notch sensitivities which range between +1 and 0 (median of 0.13); of course, these units cannot have negative notch sensitivities because their spontaneous rates are zero. DCN principal cells (types III, IV-T, and IV, filled symbols) have notch sensitivities between +1 and –1 (medians of 0.20, 0.53, and –0.33 respectively). The most sensitive notch responders, with sensitivities near -1, are all type IV units. The distribution of notch sensitivities in DCN principal cell types is actually bimodal (not shown), with one mode near 0.75 and another near –0.5. The DCN neurons with notch sensitivities near +1 are probably neurons whose notch responses are inhibitory only for wider notches. There is a range in behaviors in type IV units in terms of the notch width at which the inhibitory response appears (Spirou and Young 1991; Nelken and Young 1994); the range is not determined by BF, since neurons with the same or similar BFs can have substantially different responses at the same notch width. This diversity is illustrated by the two examples in Fig. 4.

An important point about Fig. 13D is that there is no trend with BF toward good or poor notch sensitivity. Although there are few low BF (<10 kHz) neurons in the sample, notch sensitivity appears to be as prevalent in low BF neurons as it is in high BF neurons. This result is important because it suggests that the notch sensitivity is a part of a general DCN response property and not something developed specifically for processing notches produced by the pinna, which are seen in cat at frequencies above about 8 kHz only (Musicant et al. 1990; Rice et al. 1992).

10. Targets of DCN axons in the inferior colliculus

Axons of the principal cells leave the DCN through the DAS and project to the contralateral CNIC (Osen 1972; Oliver 1984; Ryugo and Willard 1985). There they terminate in broad swaths that extend through the entire isofrequency sheet. In the decerebrate cat, neurons in the CNIC display four main response types (Ramachandran et al. 1999). One of these, called type O, appears to be particularly associated with the DCN. Type O units have tone response maps that are essentially identical to DCN type IV response maps (e.g. Fig. 14A). When inhibitory antagonists (strychnine or bicuculline) are iontophoresed at a type O recording site, the response map is unchanged for most units (Davis 1999). This result suggests that the inhibitory areas of these type O units are not created by direct inhibition within the CNIC. Evidence that these response maps are, in fact, inherited from DCN type IV units is provided by the results of blocking the contralateral DAS with lidocaine (K.A. Davis, unpublished). Blocking the output of the DCN in this way abolishes all activity in most CNIC type O units. It appears that about 70-80% of CNIC type O units inherit their tone responses from the DCN. In the remainder, iontophoresis of inhibitory antagonists abolishes most of the inhibition in the response map,

showing that some type O units are created at the level of the CNIC. The two subtypes of type O units can be distinguished by their rate responses; the discussion of this section applies only to the low-rate unit type that is associated with the DCN.

When broadband stimuli are presented, type O units differ from DCN type IV units in several ways. Most interesting are the effects of noise notches, shown in Figs. 14B and 14C. These figures show responses to broadband noise filtered to have a notch (stopband) of 3.2 kHz width centered at a range of frequencies, shown on the abscissa. The data in Fig. 14B are at a low sound level (10 dB re threshold). The type O unit gives a predominantly excitatory response to the broadband noise, with a dip in rate when the notch is centered on the unit's BF. This response is like that seen in type IV units (e.g. the example in Fig. 13B), except that the type O unit does not show an inhibitory response with the notch centered on BF. Thus the type O unit appears to receive an excitatory response to broadband stimuli which shifts up the discharge rate from the type IV input without eliminating the notch response. At higher sound levels, the response changes to that seen in Fig. 14C. At these levels, broadband noise inhibits type O units, including when the notch is centered at BF (vertical line). However, when the notch is just below BF, there is a strong excitatory response that is very specific to the location of the notch. The shift of noise responses from excitatory to inhibitory as noise level is raised is a characteristic of type O units. These units produce nonmonotonic rate functions to noise that are similar to the BF-tone rate functions of both type O units and DCN type IV units, but are more strongly nonmonotonic than type IV noise responses.

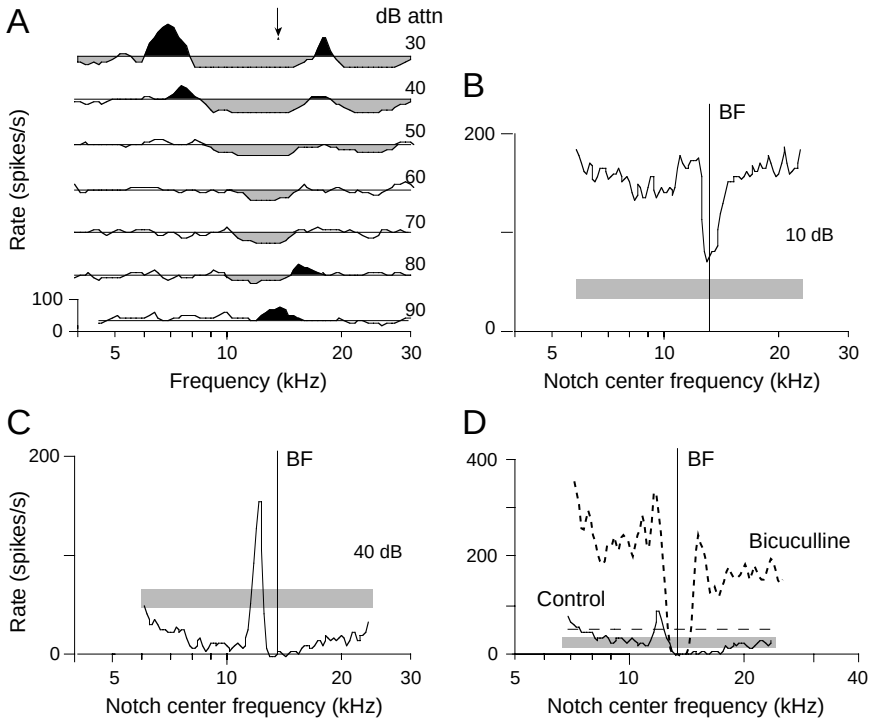

Figure 14. Some properties of a type O unit in the inferior colliculus. Neurons of this type seem to receive their primary input from DCN type IV units. A. Response map of the neuron. The arrow points to the BF. Note the features that are similar to those of type IV response maps, including the central inhibitory area, excitatory areas at threshold and at the upper frequency edge of the CIA, and the upper inhibitory sideband. B. C. Responses of the same unit to notch noise; broadband noise was filtered to have a 3.2 kHz stopband centered at various frequencies; the center frequency of the notch is given on the abscissa. The shaded bar shows the spontaneous rate and the vertical line shows BF. Data in B were obtained at about 10 dB re threshold, and data in C were obtained at about 40 dB re threshold. D. Effects of the GABA antagonist bicuculline on the responses to notches of a different type O unit. Rate versus center frequency for notch noise in control conditions (solid line) and during bicuculline iontophoresis (dashed line). The shaded bar is the spontaneous rate under control conditions and the horizontal dashed line is the spontaneous rate during bicuculline.

The relationship of the excitatory response with the notch just below BF to the response of the DCN type IV input is shown in Fig. 14D. The solid line is the response of a CNIC type O neuron to a notch, plotted against the center frequency of the notch. The same inhibitory/excitatory effect is seen, with the excitatory response occurring when the notch is just below BF. When bicuculline was iontophoresed, the same stimulus set produced the response rate shown by the dashed line. There was a large release from inhibition and the notch response became like that expected of a DCN type IV neuron; that is, there was a large excitatory response when the notch was away from BF which became inhibitory when the notch was centered on BF. Notice that the inhibitory response to the notch near BF forms the upper frequency edge of the excitatory response to the notch in the absence of bicuculline. Apparently there are strong inhibitory inputs to type O units which change the encoding of notches from an inhibitory dip at BF to an excitatory peak just below BF.

The data on the CNIC suggest two conclusions about the neural processing of sounds in the DCN. First, type IV responses clearly serve a role in the auditory system distinct from that of the more standard auditory response types in the VCN. Not only are type IV-like responses preserved in the type O population of the CNIC, but new units of this type are created by inhibitory inputs within the CNIC. Thus neurons with strong inhibitory inputs and specific non-linear responses to certain spectral shapes apparently provide a useful stimulus representation to the auditory system. This representation is not just a useful intermediate which is generated at one level and then combined into another response type at a higher level. Instead, type IV responses are themselves preserved as a parallel system at the higher level. Second, the representation of spectral notches, which is a special feature of DCN type IV units, is re-encoded in the CNIC in a different, but no less specific, format. This re-encoding depends on both excitatory and inhibitory processes, some of which are quite strong (e.g. the data in Fig. 14D). The means by which the outputs of the DCN are re-encoded in the CNIC remains as an essential piece of the DCN puzzle, necessary to the ultimate interpretation of signal representation in DCN.

11. Summary: what is the role of the DCN?

The notch responses of DCN type IV neurons demonstrate a specific sensitivity to sharp spectral features. These neurons are inhibited by spectral notches with exquisite sensitivity to the location of the notch with respect to BF. They are also inhibited by the opposite spectral feature, which is a peak in the spectrum, such as might be produced by a formant frequency in a speech sound or a resonant energy peak in the sound produced by some vibrating object. Thus DCN principal cells show a particular response, inhibition, at BFs where sharp spectral features, peaks or notches, are located in the stimulus spectrum. Sharp features of this kind often convey useful information about the environment, including the location of sound sources or the identity or quality of the sound source. Thus, it has been suggested that the DCN serves the role of identifying for the rest of the auditory system the frequencies at which interesting acoustic information is located (Nelken and Young 1996).

DCN principal cells are also predominantly inhibited by somatosensory stimuli. The most effective somatosensory stimulus seems to be stretching the muscles or tendons connected to the

pinna, as would happen when the pinna is moved away from its rest state by muscle contraction (Kanold and Young 1996). At present, it is hard to relate the somatosensory input to a useful computational mode for the animal, because the correspondence between the nature of the pinna muscle activation and the effect in DCN is not known. It is not yet clear, for example, what pinna movements would be effective in producing DCN inhibition or whether there is a mapping of specific patterns of muscle activity or pinna movement onto the array of parallel fibers. However, it is clear that movement and the position of the pinna are important sensory variables for a cat. As the cat's external ear is moved, its directional gain characteristics change dramatically (Young et al. 1996). The mapping of notch frequency into position in space, for example, moves approximately with the pinna. Thus the map in Fig. 1C applies only for the pinna in its relaxed state. In addition, movement of the pinna causes the directional transfer functions of the pinna to sweep across a stationary sound source, producing substantial time varying changes in the spectrum of the sound reaching the eardrum. Poon and Brugge (1993) showed, in an approximate simulation of this situation, that auditory nerve fibers respond strongly to the resulting spectral changes. DCN neurons would be expected to be even more sensitive to situations like transient notches in the spectrum of a sound source. In addition, a cat can substantially change its listening conditions for a particular sound source by changing the orientation of its pinnae (Young et al. 1996). The ear can be optimized for location or movement sensitivity by placing notches in the HRTF near the source or it can be optimized for identification of the source by moving the notches away (thereby eliminating the spectral distortions of the HRTF). Proper use of the information provided by the external ear requires coordination of the auditory processing of signals from the ear with the position of the pinna. The convergence of auditory and somatosensory information in the DCN thus could represent a form of sensory-motor coordination, for optimizing auditory processing. This hypothesis is similar to the hypothesized role of the cerebellum for sensory-motor coordination (Gao et al. 1996).

At the beginning of this chapter, three types of evidence for the role of a neural structure were discussed. Evidence of each of the three types has been put forward to support a role for the DCN in processing of spectral sound localization cues, and perhaps integrating them with somatosensory information important for interpreting the spectral cues. Although the evidence concerning the projection sites of the DCN's axons cannot be easily interpreted at present, it is clear that the information about spectral notches is preserved and re-encoded in the CNIC in a specifically DCN-related system. Thus we can conclude that the DCN is probably involved in some aspects of sound source localization. However, there are reasons to believe that the DCN's role extends beyond spectral sound localization cues. Among these are the fact that the specializations for notch detection are not confined to the frequency range in which notches are found in HRTFs (Fig. 13D) and the fact that there is enormous computational power in the circuitry of the molecular layer, but good hypotheses for the computations being done there have not yet emerged. Thus we have hints as to the role of the DCN, but much more to discover.

Acknowledgements. This work was supported by grants DC00023, DC00979, and DC00115 from the National Institute for Deafness and Other Communications Disorders. Thanks are due to Phyllis Taylor for preparation of figures and to our colleagues in the Johns Hopkins Center for Hearing Sciences for useful discussions of the ideas presented here. The research summarized in this chapter was done in collaboration with H.F. Voigt, W.P. Shofner, B.J. May, G.A. Spirou, I. Nelken, J.J. Rice, and P.O. Kanold.

Abbreviations

ANF	auditory nerve fiber
BBN	broadband noise
BF	best frequency
CIA	central inhibitory area
CN	cochlear nucleus
CNIC	central nucleus of the inferior colliculus
DAS	dorsal acoustic stria
DCN	dorsal cochlear nucleus
EP	evoked potential
GABA	γ-aminobutyric acid
HRTF	head-related transfer function
ILD	interaural level difference
ITD	interaural time difference
MSN	medullary somatosensory nuclei
PST	post-stimulus time
STRF	spectro-temporal receptive field
VCN	ventral cochlear nucleus
WBI	wideband inhibitor

References

Abrahams VC, Lynn B, Richmond FJ (1984a) Organization and sensory properties of small myelinated fibres in the dorsal cervical rami of the cat. J Physiol (Lond) 347:177-187.

Abrahams VC, Richmond FJ, Keane J (1984b) Projections from C2 and C3 nerves supplying muscles and skin of the cat neck: a study using transganglionic transport of horseradish peroxidase. J Comp Neurol 230:142-154.

Adams JC (1983) Multipolar cells in the ventral cochlear nucleus project to the dorsal cochlear nucleus and the inferior colliculus. Neurosci Lett 37:205-208.

Adams JC, Warr WB (1976) Origins of axons in the cat's acoustic striae determined by injection of horseradish peroxidase into severed tracts. J Comp Neurol 170:107-122.

Berrebi AS, Mugnaini E (1991) Distribution and targets of the cartwheel cell axon in the dorsal cochlear nucleus of the guinea pig. Anat Embryol 183:427-454.

Blackburn CC, Sachs MB (1990) The representation of the steady-state vowel sound /ε/ in the discharge patterns of cat anteroventral cochlear nucleus neurons. J Neurophysiol 63:1191-1212.

Blackstad TW, Osen KK, Mugnaini E (1984) Pyramidal neurones of the dorsal cochlear nucleus: A Golgi and computer reconstruction study in cat. Neuroscience 13:827-854.

Blum JJ, Reed MC (1998) Effects of wide band inhibitors in the dorsal cochlear nucleus. II. Model calculations of the responses to complex tones. J Acoust Soc Am 103:2000-2009.

Blum JJ, Reed MC, Davies JM (1995) A computational model for signal processing by the dorsal cochlear nucleus. II. Responses to broadband and notch noise. J Acoust Soc Am 98:181-191.

Burian M, Gestoettner W (1988) Projection of primary vestibular afferent fibres to the cochlear nucleus in the guinea pig. Neurosci Lett 84:13-17.

Cant NB (1992) The cochlear nucleus: Neuronal types and their synaptic organization. In: Webster DB, Popper AN, Fay RR (eds) The Mammalian Auditory Pathway: Neuroanatomy. Berlin: Springer-Verlag, pp. 66-116.

Cariani PA, Delgutte B (1996a) Neural correlates of the pitch of complex tones. I. Pitch and pitch salience. J Neurophysiol 76:1698-1716.

Cariani PA, Delgutte B (1996b) Neural correlates of the pitch of complex tones. II. Pitch shift, pitch ambiguity, phase invariance, pitch circularity, rate pitch, and the dominance region for pitch. J Neurophysiol 76:1717-1734.

Caspary DM, Pazara KE, Kossl M, Faingold CL (1987) Strychnine alters the fusiform cell output from the dorsal cochlear nucleus. Brain Res 417:273-282.

Dabak AG, Johnson DH (1992) Function-based modeling of binaural processing: interaural phase. Hear Res 58:200-212.

Davis KA (1999) The basic receptive field properties of neurons in the inferior colliculus of decerebrate cats are rarely created by local inhibitory mechanisms. Soc Neurosci Abstr 25:667.

Davis KA, Young ED (1997) Granule cell activation of complex-spiking neurons in dorsal cochlear nucleus. J Neurosci 17:6798-6806.

Davis KA, Young ED (2000) Pharmacological evidence of inhibitory and disinhibitory neural circuits in dorsal cochlear nucleus. J Neurophysiol 83:926-940.

Davis KA, Ding J, Benson TE, Voigt HF (1996a) Response properties of units in the dorsal cochlear nucleus of unanesthetized decerebrate gerbil. J Neurophysiol 75:1411-1431.

Davis KA, Miller RL, Young ED (1996b) Effects of somatosensory and parallel-fiber stimulation on neurons in dorsal cochlear nucleus. J Neurophysiol 76:3012-3024.

Doucet JR, Ryugo DK (1997) Projections from the ventral cochlear nucleus to the dorsal cochlear nucleus in rats. J Comp Neurol 385:245-264.

Doucet JR, Ross AT, Gillespie MB, Ryugo DK (1999) Glycine immunoreactivity of multipolar neurons in the ventral cochlear nucleus which project to the dorsal cochlear nucleus. J Comp Neurol 408:515-531.

Evans EF, Nelson PG (1973) The responses of single neurons in the cochlear nucleus of the cat as a function of their location and the anaesthetic state. Exp Brain Res 17:402-427.

Evans EF, Zhao W (1993) Varieties of inhibition in the processing and control of processing in the mammalian cochlear nucleus. Prog in Brain Res 97:117-126.

Fernandez C, Karapas F (1967) The course and termination of the striae of Monakow and Held in the cat. J Comp Neurol 131:371-386.

Gao J-H, Parsons LM, Bower JM, Xiong J, Li J, Fox PT (1996) Cerebellum implicated in sensory acquisition and discrimination rather than motor control. Science 272:545-547.

Golding NL, Oertel D (1997) Physiological identification of the targets of cartwheel cells in the dorsal cochlear nucleus. J Neurophysiol 78:248-260.

Hancock KE, Davis KA, Voigt HF (1997) Modeling inhibition of type II units in dorsal cochlear nucleus. Biol Cybern 76:419-428.

Hekmatpanah J (1961) Organization of tactile dermatomes, C_1 through L_4, in cat. J Neurophysiol 24:129-140.

Huang AY, May BJ (1996a) Sound orientation behavior in cats. II. Mid-frequency spectral cues for sound localization. J Acoust Soc Am 100:1070-1080.

Huang AY, May BJ (1996b) Spectral cues for sound localization in cats: Effects of frequency domain on minimum audible angles in the median and horizontal planes. J Acoust Soc Am 100:2341-2348.

Imig TJ, Samson F (2000) Differential projection of dorsal and intermediate acoustic striae upon fields AAF and AI in cat auditory cortex. Abstr Assoc Res Otolaryngol 23:11.

Imig TJ, Poirier P, Irons WA, Samson FK (1997) Monaural spectral contrast mechanism for neural sensitivity to sound direction in the medial geniculate body of the cat. J Neurophysiol 78:2754-2771.

Imig TJ, Bibikov NG, Poirier P, Samson FK (2000) Directionality derived from pinna-cue spectral notches in cat dorsal cochlear nucleus. J Neurophysiol 83:907-925.

Itoh K, Kamiya H, Mitani A, Yasui Y, Takada M, Mizuno N (1987) Direct projection from the dorsal column nuclei and the spinal trigeminal nuclei to the cochlear nuclei in the cat. Brain Res 400:145-150.

Jiang D, Palmer AR, Winter IM (1996) Frequency extent of two-tone facilitation in onset units in the ventral cochlear nucleus. J Neurophysiol 75:380-395.

Joris PX (1998) Response classes in the dorsal cochlear nucleus and its output tract in the chloralose-anesthetized cat. J Neurosci 18:3955-3966.

Kanold PO, Young ED (1996) Deep somatosensory receptors associated with the pinna provide static inhibition of principal neurons in the cat dorsal cochlear nucleus (DCN). Abstr Assoc Res Otolaryngol 19:170.

Kanold PO, Young ED (1998) Somatosensory inputs to the cat dorsal cochlear nucleus (DCN) derives primarily from spinal nerve C2. Abstr Assoc Res Otolaryngol 21:98.

Kavanagh GL, Kelly JB (1992) Midline and lateral field sound localization in the ferret (Mustela putorius): Contribution of the superior olivary complex. J Neurophysiol 67:1643-1658.

Kevetter GA, Perachio AA (1989) Projections from the sacculus to the cochlear nuclei in the Mongolian Gerbil. Brain, Behav and Evol 34:193-200.

Kuhn GF (1987) Physical acoustics and measurements pertaining to directional hearing. In: Yost WA, Gourevitch G (eds) Directional Hearing. Berlin: Springer-Verlag, pp. 3-25.

Lingenhöhl K, Friauf E (1994) Giant neurons in the rat reticular formation: A sensorimotor interface in the elementary acoustic startle circuit? J Neurosci 14:1176-1194.

Lorente de Nó R (1981) The Primary Acoustic Nuclei. New York: Raven Press.

Manis PB (1989) Responses to parallel fiber stimulation in the guinea pig dorsal cochlear nucleus in vitro. J Neurophysiol 61:149-161.

Manis PB, Spirou GA, Wright DD, Paydar S, Ryugo DK (1994) Physiology and morphology of complex spiking neurons in the guinea pig dorsal cochlear nucleus. J Comp Neurol 348:261-276.

Mast TE (1970) Binaural interaction and contralateral inhibition in dorsal cochlear nucleus of the chinchilla. J Neurophysiol 33:108-115.

Masterton RB, Granger EM (1988) Role of the acoustic striae in hearing: contribution of dorsal and intermediate striae to detection of noises and tones. J Neurophysiol 60:1841-1860.

Masterton RB, Granger EM, Glendenning KK (1994) Role of acoustic striae in hearing--mechanism for enhancement of sound detection in cats. Hear Res 73:209-222.

May BJ (2000) Role of the dorsal cochlear nucleus in the sound localization behavior of cats. Hear Res (in press).

May BJ, Huang A, LePrell G, Hienz RD (1996) Vowel formant frequency discrimination in cats: Comparison of auditory nerve representations and psychophysical thresholds. Aud Neurosci 3:135-162.

Meloni EG, Davis M (1998) The dorsal cochlear nucleus contributes to a high intensity component of the acoustic startle reflex in rats. Hear Res 119:69-80.

Merchán MA, Collia FP, Merchán JA, Saldaña E (1985) Distribution of primary afferent fibres in the cochlear nuclei. A silver an horseradish peroxidase (HRP) study. J Anat 141:121-130.

Middlebrooks JC, Green DM (1991) Sound localization by human listeners. Ann Rev Psychol 42:135-159.

Mugnaini E (1985) GABA neurons in the superficial layers of rat dorsal cochlear nucleus: light and electron microscopic immunocytochemistry. J Comp Neurol 235:537-570.

Mugnaini E, Osen KK, Dahl AL, Friedrich Jr. VL, Korte G (1980a) Fine structure of granule cells and related interneurons (termed Golgi cells) in the cochlear nuclear complex of cat, rat, and mouse. J Neurocytol 9:537-570.

Mugnaini E, Warr WB, Osen KK (1980b) Distribution and light microscopic features of granule cells in the cochlear nuclei of cat, rat, and mouse. J Comp Neurol 191:581-606.

Musicant AD, Chan JCK, Hind JE (1990) Direction-dependent spectral properties of cat external ear: New data and cross-species comparisons. J Acoust Soc Am 87:757-781.

Nelken I, Young ED (1994) Two separate inhibitory mechanisms shape the responses of dorsal cochlear nucleus type IV units to narrowband and wideband stimuli. J Neurophysiol 71:2446-2462.

Nelken I, Young ED (1996) Why do cats need a dorsal cochlear nucleus? Rev Clinical and Basic Pharmacology 7:199-220.

Nelken I, Young ED (1997) Linear and non-linear spectral integration in type IV neurons of the dorsal cochlear nucleus: I. Regions of linear interaction. J Neurophysiol 78:790-799.

Nelken I, Kim PJ, Young ED (1997) Linear and non-linear spectral integration in type IV neurons of the dorsal cochlear nucleus: II. Predicting responses using non-linear methods. J Neurophysiol 78:800-811.

Oertel D, Wickesberg RE (1993) Glycinergic inhibition in the cochlear nuclei: evidence for tuberculoventral neurons being glycinergic. In: Merchán MA, Juiz JM, Godfrey DA, Mugnaini E (eds) The Mammalian Cochlear Nuclei: Organization and Function. New York: Plenum, pp. 225-237.

Oertel D, Wu SH, Garb MW, Dizack C (1990) Morphology and physiology of cells in slice preparations of the posteroventral cochlear nucleus of mice. J Comp Neurol 295:136-154.

Ohlrogge M, Doucet J, Rose L, Ryugo D (2000) Projections from the pontine nuclei to the cochlear nucleus in rats. Abstr Assoc Res Otolaryngol 23:37.

Oliver DL (1984) Dorsal cochlear nucleus projections to the inferior colliculus in the cat: A light and electron microscopic study. J Comp Neurol 224:155-172.

Osen KK (1969) Cytoarchitecture of the cochlear nuclei in the cat. J Comp Neurol 136:453-482.

Osen KK (1970) Course and termination of the primary afferents in the cochlear nuclei of the cat. Arch Ital Biol 108:21-51.

Osen KK (1972) Projection of the cochlear nuclei on the inferior colliculus in the cat. J Comp Neurol 144:355-372.

Osen KK (1983) Orientation of dendritic arbors studied in Golgi sections of the cat dorsal cochlear nucleus. In: Webster WR, Aitkin LM (eds) Mechanisms of Hearing. Clayton: Monash Univ Press, pp. 83-89.

Osen KK, Ottersen OP, Storm-Mathisen J (1990) Colocalization of glycine-like and GABA-like immunoreactivities. A semiquantitative study of individual neurons in the dorsal cochlear nucleus of cat. In: Ottersen OP, Storm-Mathisen J (eds) Glycine Neurotransmission. New York: John Wiley and Sons, pp. 417-451.

Ostapoff EM, Morest DK, Potashner SJ (1990) Uptake and retrograde transport of [3H]GABA from the cochlear nucleus to the superior olive in the guinea pig. J Chem Neuroanat 3:285-289.

Ostapoff EM, Benson CG, Saint Marie RL (1997) GABA- and glycine-immunoreactive projections from the superior olivary complex to the cochlear nucleus in guinea pig. J Comp Neurol 381:500-511.

Palmer AR, Jiang D, Marshall DH (1996) Responses of ventral cochlear nucleus onset and chopper units as a function of signal bandwidth. J Neurophysiol 75:780-794.

Parham K, Kim DO (1995) Spontaneous and sound-evoked discharge characteristics of complex-spiking neurons in the dorsal cochlear nucleus of the unanesthetized decerebrate cat. J Neurophysiol 73:550-561.

Poon PWF, Brugge JF (1993) Sensitivity of auditory nerve fibers to spectral notches. J Neurophysiol 70:655-666.

Populin LC, Yin TCT (1998) Behavioral studies of sound localization in the cat. J Neurosci 18:2147-2160.

Ramachandran R, Davis KA, May BJ (1999) Single-unit responses in the inferior colliculus of decerebrate cats I. Classification based on frequency response maps. J Neurophysiol 82:152-163.

Reed MC, Blum JJ (1995) A computational model for signal processing by the dorsal cochlear nucleus, I: responses to pure tones. J Acoust Soc Am 97:425-438.

Rhode WS (1999) Vertical cell responses to sound in cat dorsal cochlear nucleus. J Neurophysiol 82:1019-1032.

Rhode WS, Greenberg S (1992) Physiology of the cochlear nucleus. In: Popper AN, Fay RR (eds) The Mammalian Auditory Pathway: Neurophysiology. Berlin: Springer-Verlag, pp. 94-152.

Rhode WS, Kettner RE (1987) Physiological studies of neurons in the dorsal and posteroventral cochlear nucleus of the unanesthetized cat. J Neurophysiol 57:414-442.

Rhode WS, Smith PH, Oertel D (1983) Physiological response properties of cells labeled intracellularly with horseradish peroxidase in cat dorsal cochlear nucleus. J Comp Neurol 213:426-447.

Rice JJ, May BJ, Spirou GA, Young ED (1992) Pinna-based spectral cues for sound localization in cat. Hear Res 58:132-152.

Rice JJ, Young ED, Spirou GA (1995) Auditory-nerve encoding of pinna-based spectral cues: Rate representation of high-frequency stimuli. J Acoust Soc Am 97:1764-1776.

Richter JA, Holtman JR (1982) Barbiturates: their in vivo effects and potential biochemical mechanisms. Neurobiol 18:275-319.

Roberts RC, Ribak CE (1987) GABAergic neurons and axon terminals in the brainstem auditory nuclei of the gerbil. J Comp Neurol 258:267-280.

Roth GL, Kochhar RK, Hind JE (1980) Interaural time differences: Implications regarding the neurophysiology of sound localization. J Acoust Soc Am 68:1643-1651.

Ryugo DK, May SK (1993) The projections of intracellularly labeled auditory nerve fibers to the dorsal cochlear nucleus of cats. J Comp Neurol 329:20-35.

Ryugo DK, Willard FH (1985) The dorsal cochlear nucleus of the mouse: A light microscopic analysis of neurons that project to the inferior colliculus. J Comp Neurol 242:381-396.

Saadé NE, Frangieh AS, Atweh SF, Jabbur SJ (1989) Dorsal column input to cochlear neurons in decerebrate-decerebellate cats. Brain Res 486:399-402.

Sachs MB, Abbas PJ (1974) Rate versus level functions for auditory-nerve fibers in cats: tone-burst stimuli. J Acoust Soc Am 56:1835-1847.

Saint Marie RL, Benson CG, Ostapoff EM, Morest DK (1991) Glycine immunoreactive projections from the dorsal to the anteroventral cochlear nucleus. Hear Res 51:11-28.

Samson FK, Clarey JC, Barone P, Imig TJ (1993) Effects of ear plugging on single-unit azimuth sensitivity in cat primary auditory cortex. I. Evidence for monaural directional cues. J Neurophysiol 70:492-511.

Schalk T, Sachs MB (1980) Nonlinearities in auditory-nerve fiber response to bandlimited noise. J Acoust Soc Am 67:903-913.

Shofner WP, Young ED (1985) Excitatory/inhibitory response types in the cochlear nucleus: Relationships to discharge patterns and responses to electrical stimulation of the auditory nerve. J Neurophysiol 54:917-939.

Smith PH, Rhode WS (1989) Structural and functional properties distinguish two types of multipolar cells in the ventral cochlear nucleus. J Comp Neurol 282:595-616.

Spirou GA, Young ED (1991) Organization of dorsal cochlear nucleus type IV unit response maps and their relationship to activation by bandlimited noise. J Neurophysiol 65:1750-1768.

Spirou GA, Davis KA, Nelken I, Young ED (1999) Spectral integration by type II interneurons in dorsal cochlear nucleus. J Neurophysiol 82:648-663.

Sutherland DP, Glendenning KK, Masterton RB (1998a) Role of acoustic striae in hearing: Discrimination of sound-source elevation. Hear Res 120:86-108.

Sutherland DP, Masterton RB, Glendenning KK (1998b) Role of acoustic striae in hearing: reflexive responses to elevated sound-sources. Behav Brain Res 97:1-12.

van Adel BA, Kelly JB (1998) Kainic acid lesions of the superior olivary complex: Effects on sound localization by the albino rat. Behav Neurosci 112:432-446.

Voigt HF, Young ED (1980) Evidence of inhibitory interactions between neurons in the dorsal cochlear nucleus. J Neurophysiol 44:76-96.

Voigt HF, Young ED (1990) Cross-correlation analysis of inhibitory interactions in dorsal cochlear nucleus. J Neurophysiol 64:1590-1610.

Waller HJ, Godfrey DA, Chen K (1996) Effects of parallel fiber stimulation on neurons of rat dorsal cochlear nucleus. Hear Res 98:169-179.

Weedman DL, Ryugo DK (1996) Projections from auditory cortex to the cochlear nucleus in rats: Synapses on granule cell dendrites. J Comp Neurol 371:311-324.

Weedman DL, Pongstaporn T, Ryugo DK (1996) Ultrastructural study of the granule cell domain of the cochlear nucleus in rats: Mossy fiber endings and their targets. J Comp Neurol 369:345-360.

Weinberg RJ, Rustioni A (1987) A cuneocochlear pathway in the rat. Neurosci 20:209-219.

Winter IM, Palmer AR (1995) Level dependence of cochlear nucleus onset unit responses and facilitation by second tones or broadband noise. J Neurophysiol 73:141-159.

Wouterlood FG, Mugnaini E, Osen KK, Dahl A-L (1984) Stellate neurons in rat dorsal cochlear nucleus studied with combined Golgi impregnation and electron microscopy: synaptic connections and mutual coupling by gap junctions. J Neurocytol 13:639-664.

Wright DD, Ryugo DK (1996) Mossy fiber projections from the cuneate nucleus to the dorsal cochlear nucleus of rat. J Comp Neurol 365:159-172.

Young ED (1980) Identification of response properties of ascending axons from dorsal cochlear nucleus. Brain Res 200:23-38.

Young ED (1998) The cochlear nucleus. In: Shepherd GM (ed) Synaptic Organization of the Brain. New York: Oxford Press, pp. 121-157.

Young ED, Brownell WE (1976) Responses to tones and noise of single cells in dorsal cochlear nucleus of unanesthetized cats. J Neurophysiol 39:282-300.

Young ED, Voigt HF (1981) The internal organization of the dorsal cochlear nucleus. In: Syka J, Aitkin L (eds) Neuronal Mechanisms of Hearing. New York: Plenum, pp. 127-133.

Young ED, Voigt HF (1982) Response properties of type II and type III units in dorsal cochlear nucleus. Hear Res 6:153-169.

Young ED, Spirou GA, Rice JJ, Voigt HF (1992) Neural organization and responses to complex stimuli in the dorsal cochlear nucleus. Phil Trans R Soc Lond B 336:407-413.

Young ED, Nelken I, Conley RA (1995) Somatosensory effects on neurons in dorsal cochlear nucleus. J Neurophysiol 73:743-765.

Young ED, Rice JJ, Tong SC (1996) Effects of pinna position on head-related transfer functions in the cat. J Acoust Soc Am 99:3064-3076.

Young ED, Rice JJ, Spirou GA, Nelken I, Conley RA (1997) Head-related transfer functions in cat: neural representation and the effects of pinna movement. In: Gilkey RH, Anderson TR (eds) Binaural and Spatial Hearing in Real and Virtual Environments. Mahwah, NJ: Lawrence Erlbaum Assoc, pp. 475-498.

Yu JJ, Young ED (2000) Linear and nonlinear pathways of spectral information transmission in the cochlear nucleus. Proc Nat Acad Sci (in press).

Zhang S, Oertel D (1993a) Cartwheel and superficial stellate cells of the dorsal cochlear nucleus of mice: Intracellular recordings in slices. J Neurophysiol 69:1384-1397.

Zhang S, Oertel D (1993b) Tuberculoventral cells of the dorsal cochlear nucleus of mice: Intracellular recordings in slices. J Neurophysiol 69:1409-1421.